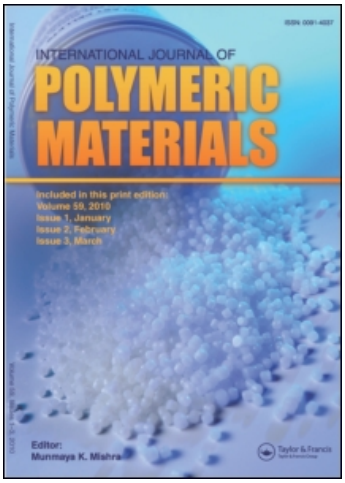

International Journal of Polymeric Materials
Publication details, including instructions for authors and subscription information:
http://www.informaworld.com/smpp/title~content=t713647664

Effects of Magnetic Fields on Polymer Liquid Crystals

E. Lizuka[a]
[a] Department of Functional Polymer Science, Faculty of Textile Science and Technology, Shinshu University, Nagano, Japan

To cite this Article Lizuka, E.(2000) 'Effects of Magnetic Fields on Polymer Liquid Crystals', International Journal of Polymeric Materials, 45: 3, 191 — 238
To link to this Article: DOI: 10.1080/00914030008035045
URL: http://dx.doi.org/10.1080/00914030008035045

Intern. J. Polymeric Mater., 2000, Vol. 45, pp. 191–238
Reprints available directly from the publisher
Photocopying permitted by license only

Effects of Magnetic Fields on Polymer Liquid Crystals

E. LIZUKA

Department of Functional Polymer Science, Faculty of Textile Science and Technology, Shinshu University, Ueda, Nagano 386, Japan

(Received 18 December 1998)

The effects of magnetic fields on polymer liquid crystals (PLCs) are analyzed, dealing in turn with isotropic solutions, lyotropic LCs (including polypeptides, polyribonucleotides and DNA) and thermotropic PLCs (including polyesters and polypeptides). Looking for a common denominator in LC behavior, living systems are also analyzed, including viruses, biological membranes, sperm nuclei, rhodopsin and fibrinogen. Magnetropism is discussed, as are applications of PLC oriented in magnetic fields for the purpose of producing ultra-high modulus materials.

Keywords: Magnetic fields; polymer liquid crystals; PLCs; isotropic liquid crystal solutions; lyotropic liquid crystals, polypeptides; polyribonucleotides; DNA; polyesters; polypeptides; viruses; biological membranes; sperm nuclei; rhodopsin; fibrinogen; magnetropism; ultra-high modulus polymers

1. INTRODUCTION

Finding the ability of polymer molecules to form oriented macrostructures in solution were made first with poly(γ-benzyl *L*-glutamate) (PBLG) by Elliott and Ambrose [1]. Robinson *et al.* [2–4] revealed that they are a cholesteric structure and the feature of the liquid crystals of this polypeptide were made clear by them. According to Gray [5], the basis for Flory's theory [6] that predicts the formation of rod-like polymer liquid crystals lies in the energy requirements for polymer molecules, which resist bending, arranged randomly in solution. At some critical concentration, additional polymer molecules go into a disordered solution only in the high energy (bent) conformation to

accommodate the space available to them. In the absence of any other driving force, the polymer molecules will spontaneously form an ordered phase in which the polymer molecules are fully extended and parallel. Double or triple stranded helices of polyribonucleotides including DNA thus form liquid crystals in solution.

In liquid-crystalline state, all these polymer molecules respond to external stimuli such as electric and magnetic fields with high sensitivity; however, polymer liquid crystals have not come into use in the field of opto-electronics because of their rather long response time unlike monomer liquid crystals. Liquid crystals that include DNA or/and polypeptides are building blocks for living systems [7] and their functions, some of which are in connection with electric-and magnetic-phenomena, are owing highly to the specific characteristic of liquid crystals. Information concerning the magnetic effects of polymer liquid crystals will lead to their future application to biological field.

These polymer liquid crystals are lyotropic and the liquid crystal spinning is a newly developed technique to produce high modulus fibers. In an attempt to increase the glass transition temperature of poly (ethylene telephthalate) (PET) and its flame resistance, Jackson and Kuhfuss [8] increased the aromatic character of the polyester by modifying it with *p*-hydroxybenzoic acid (PHB). They found that polyesters with a PHB content of 35 mol% (PET/0.35PHB) had opaque melts and that minimum melt viscosities were obtained with polyesters containing 60 – 70 mol% PHB. The polyesters became amenable to injection moulding and some of the injection-moulded fibers had properties superior to commercial glass fiber reinforced polyesters. These copolyesters satisfied descriptions of liquid crystals of the cholesteric type and McFarlane *et al.* [9] suggested that they were the first thermotropic liquid-crystalline polymers to be recognized. The finding of thermotropic polymer liquid crystals has led to the usage of magnetic field to produce materials which show elastic modulus much higher than that shown by injection-moulded materials.

2. ISOTROPIC SOLUTION

Diamagnetically anisotropic small molecules in fluid state is known to orient in an external magnetic field H (Cotton-Mouton effect). Partial

orientation takes place in thermal equilibrium and the degree of orientation β is described, assuming a rigid rod and according to the Boltzmann statistics, in the form [10],

$$\beta = (\chi_{\parallel} - \chi_{\perp})H^2/kT \tag{1}$$

where $\chi_{\parallel}$ and $\chi_{\perp}$ are the absolute susceptibility values parallel and perpendicular to the rod axis, k is the Boltzmann constant and T is the absolute temperature and $\beta \ll 1$.

At room temperature and conventionally available magnetic fields ($H \sim 1\,\mathrm{T}$), the magnitude of β for single, even strongly anisotropic molecules like benzene ($\chi_{\parallel} - \chi_{\perp} = 60 \times 10^{-6}$ emu/mol; $1\,\mathrm{J/T^2} = 10^{-1}\,\mathrm{erg/gauss^2}$, or 10^{-1} emu) is very small ($\beta \sim 10^{-7}$) [11]. However, β can be drastically increased when a large number of such molecules form a molecular cluster in which they are rigidly fixed together parallel to one another as in the case of liquid crystals of polypeptides. The degree of orientation is then proportional to the number of the molecules, N,

$$\beta = N(\chi_{\parallel} - \chi_{\perp})H^2/kT \tag{2}$$

Maret *et al.* [10] also have dealt with the magnetic-field orientation of flexible polymers. The degree of orientation then turns to:

$$\beta = (2P/l_0)(\chi_{\parallel} - \chi_{\perp})H^2/kT \tag{3}$$

where P is the Kratky-Porod persistence length and l_0 is the length of one monomer. For small degrees of orientation, the magnetically induced birefringence Δn_H is proportional to β, to the anisotropy of the molecular optical polarizability $\alpha_{\parallel} - \alpha_{\perp}$, and to the polymer concentration c; $\Delta n_H \propto (\alpha_{\parallel} - \alpha_{\perp})\beta c$, or by introducing the Cotton-Mouton constant [12] C_M,

$$\Delta n_H = n_{\parallel} - n_{\perp} = C_M \lambda H^2 \tag{4}$$

where $n_{\parallel}$ and $n_{\perp}$ are the refractive indices parallel and perpendicular to the applied magnetic field H, respectively, λ is the wavelength of light. The persistence length can be determined by comparing Δn_H with the birefringence of a fully aligned polymer sample, Δn_{sat} and using the

relation,

$$\Delta n_H/\Delta n_{\text{sat}} = (1/6)\beta \tag{5}$$

or by the ratio of the monomeric and polymeric Cotton-Mouton constant, $C_M(\text{mono})/C_M(\text{poly}) = 2P/l_0$ [10].

Maret *et al.* [10, 11] have measured the magnetic birefringence of the aqueous solution of DNA, poly (A), poly (A + U), or of several other polyribonucleotides using a photoelastic modulation technique. Even at fields up to 13 T, the magnetically induced birefringence is strictly linear in H^2; however, the value of Δn_H at 12 T is only 2.31×10^{-7} for high-molecular weight calfthymus DNA (concentration $c \cong 10$ mg/ml (1kg/l = 10^3 mg/ml)). The alignment of DNA molecules can be produced by shearing the solution between two glass plates of 0.6 mm distance and the birefringence is measured as a function of the relative shear velocity up to 10 mm/sec where saturation Δn is almost reached. The extraporated value $\Delta n_{\text{sat}} = 1.57 \times 10^{-4}$ for $c = 10$ mg/ml leads to the small degree of orientation $\beta = 0.88\%$ in $H = 12$ T. From the signs of Δn they have concluded that DNA tends to orient with the filament axis in the plane perpendicular to magnetic field.

The diamagnetic anisotropy of the base pairs has been calculated to exceed that of benzene, 9.48×10^{-21} erg/T^2 (1 J/T^2 = 10^7 erg/T^2), by a factor of 1.098 and 0.827 for adenine-thymine (A-T) and guanine-cytosine (G-C), respectively [13]. With the known base composition of calf thymus DNA ($f_{GC} = 0.42$) and taking $l_0 = 3.4$ Å and $P = (1/2)\, l_0 N$, Maret *et al.* [1] have found that $P = 445$ Å and $N = 262$ using Eq. (3).

3. LYOTROPIC LIQUID CRYSTALS

3.1. Polypeptides

The formation of oriented macrostructure is the result of appearance of discontinuities in the chemical potentials at a certain polymer concentration where they become minimum. According to Flory [6]. This critical concentration, v_2^* is given in the form:

$$v_2^* = (8/p)(1 - 2/p) \tag{6}$$

where p is the axis ratio and this equation holds good in a liquid-crystalline solution of PBLG,

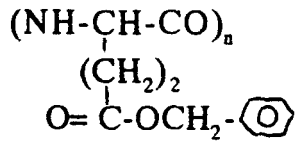

dissolved in *m*-cresol [14]. The birefringent phase appears at this concentration which was named A-point by Robinson *et al.* [3]. Above this concentration two phases, isotropic and birefringent, exist in equilibrium; the birefringent phase dispersed in the isotropic phase forms spherulites owing to the interfacial tension between the two phases. Above a still higher concentration, B-point, only the birefringent phase can exist and forms a continuous cholesteric structure [2–4].

(a) Orientation

When a liquid crystalline solution of PBLG in methylene halides is placed in the magnetic field of a high resolution NMR spectrometer, the signals of the solvent molecules split into multiplet [15–19]. This is the case also in poly (γ-ethyl *L*-glutamate) (PELG) as shown in Figure 1 [20] and indicates that liquid crystals of polypeptides tend to orient in the direction of an applied magnetic field. The highly dielectric solvent molecules are aligned in the same direction owing to effects of electric dipole–dipole interactions between the solvent molecules and the oriented polymer molecules. Interatomic vectors of the proton pairs of the solvent molecule take a certain angle to the direction of the applied field, and thereby the direct dipole–dipole interactions split the methylene signal into a doublet [15]. The separation h due to the dipole–dipole interaction for a pair of protons, in motion about an axis perpendicular to the interatomic axis, was given by Gutowsky and Pake [21] as

$$h = (3/2)\mu d^{-3}(1 - 3\cos^2\theta) \tag{7}$$

where μ is the magnetic moment of the proton (2.79 nuclear magneton), d is the interatomic distance of a pair of protons (1.8 Å)

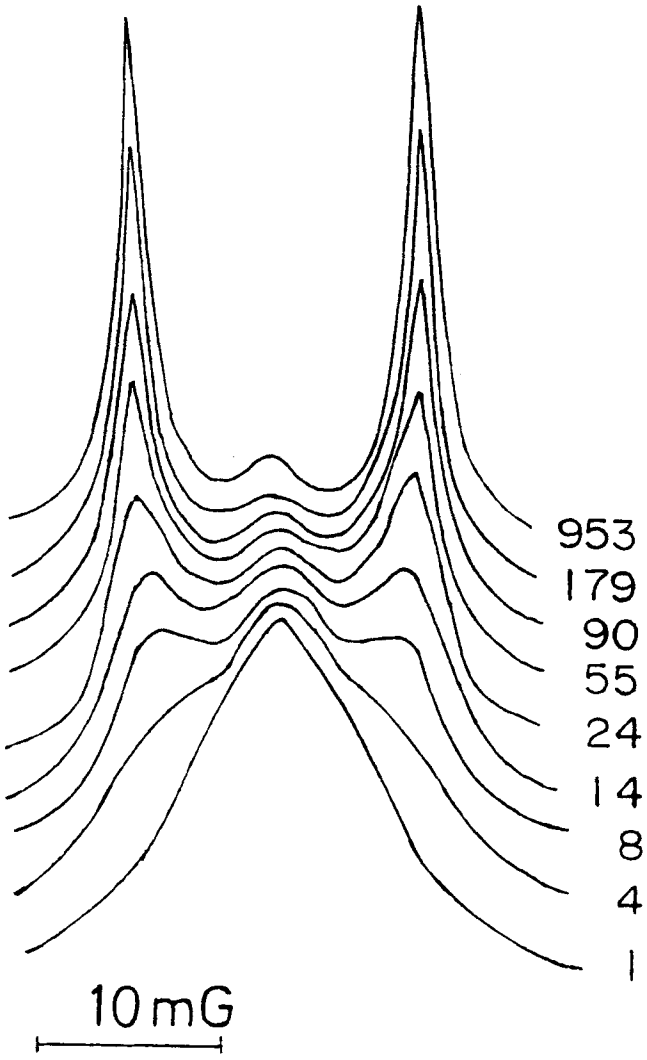

FIGURE 1 Time dependence of the NMR spectra of a liquid-crystalline solution in the magnetic field (1.4 T) of a high resolution NMR spectrometer for PELG (degree of polymerization $r \cong 1{,}500$) in methylene chloride. Polymer concentration, 14.0 vol%. The numbers near the curves give the number in minutes.

and θ is the angle between the axis of rotation of the methylene group and the direction of the magnetic field. Sobajima [15] has measured the separation of the doublet after the sample solution reached the steady-

state orientation by changing the angle α, between the initial direction of sample orientation and the direction of the applied field, α being identical with θ. He has found that the separation follows Eq. (2) well in the dependence on the angle; however, the magnitude of maximum separation observed at $\theta = 0°$ is far smaller than the expected value of 7.3 gauss (1 T = 10^4 gauss). Incidentally the separation is 2 through 6 gauss (full separation) in low molecular-weight compounds such as *p*-azoxyanisole and *p*-azoxyphenetol [22–24] and the deviation from the calculated value can be interpreted by the degree of orientation.

In order to explain the big difference between the observed and the calculated separation, Sobajima [15] has assumed the fluctuation of the rotation axes of the solvent molecules due to thermal energy and has rewritten Eq. (2) as follows:

$$h = (3/2)\mu r^{-3}(1 - 3\cos^2\varphi)(1/2)\langle 1 - 3\cos^2\alpha\rangle_{\mathrm{AV}} \tag{8}$$

where φ is the angle between the molecular axis of PBLG and the magnetic-field direction and α, the angle between the axis of rotation of the methylene group and the molecular axis of the polymer. The potential energy U of a methylene halide molecule in a molecular field arising from the dipole moment of the oriented polymer molecules E is given by $U = -pE\cos\alpha$, where p is the electric dipole moment of the methylene halide molecule. According to the Boltzmann distribution law, he has shown that the separation can be given finally in the form,

$$h = (1/10)\mu r^{-3}(1 - 3\cos^2\varphi)(pE/kT)^2 \tag{9}$$

where k and T have their usual meanings. The validity of this new equation can be confirmed by the temperature dependence of the separation. The value of E at the position of the methylene halide molecule has been calculated as 5.6×10^3 C.G.S.e.s.u. (1 V/m = 0.333×10^{-4} CGS esu) using $p = 1.62$ Debye (1 Debye = 3×10^{-29} C · m) for methylene chloride.

The orientation of polypeptides in a magnetic field has been detected directly by measurements of the birefringence or of the infrared dichroic ratio of liquid-crystalline solution at 3,300 cm^{-1} which is the center of the NH stretching vibration mode of polypeptides [20, 25]. The solution is put in a quartz cell of path length 1 mm with a quartz

spacer inside to adjust the path length to 0.05–0.10 mm. The quartz cell with sample solution is then put between the poles of a permanent magnet (of 0.75 T) placed in the sample house of an infrared spectrophotometer. Percent transmission of the solution is read with the electric vector of the light in turn parallel and perpendicular to the direction of the magnetic field. The direction of the magnetic field is designed to tilt by 45 degrees with respect to the entrance slit of the spectrophotometer in order to eliminate the error in the observed dichroic ratio due to the polarization of the monochrometer. The direction of the transition moment in question makes a fixed angle γ of 29° with the molecular axis in the α-helical state [26]. Therefore, it is parallel rather than perpendicular to the molecular axis and the order parameter s can be obtained, according to the Boltzmann distribution law, in the form [27, 28],

$$\begin{aligned} s &= (1/2)(3\langle\cos^2\theta\rangle_{AV} - 1) \\ &= [2/(2 - 3\sin^2\gamma)] \cdot [\{(D_\parallel/D_\perp) - 1\}/\{(D_\parallel/D_\perp) + 2\}] \end{aligned} \tag{10}$$

where θ is the angle that the molecular axis makes with respect to the direction of the external field. $D_\parallel$ and $D_\perp$ are absorbances of light polarized parallel and perpendicular to the magnetic field, respectively.

Both the dichroic ratio $D_\parallel/D_\perp$ and birefringence are time dependent and suggest that the polymer helices align parallel to the direction of magnetic field with time. Figure 2 shows that the rate of ordering and steady-state birefringence depend on various factors such as the polymer concentration, degree of polymerization r of the specimen, solvent used et cetera [29]. A time lag may be observed in some cases and the birefringence increases in two steps. The first step is supposedly indicative of the presence and overcome of wall effects. The degree of orientation does not change when the direction of magnetic field is reversed after the steady-state orientation is reached, which suggests that the magnetic-field orientation is due to the induced magnetic dipole of the polypeptide molecule.

The peptide group, —NH · CO—, of a polypeptide molecule has a permanent electric dipole moment of about 6 Debye. As shown in Figure 3, all the dipoles point roughly in the same direction in the α-helical conformation and the polymer molecule has a resultant large

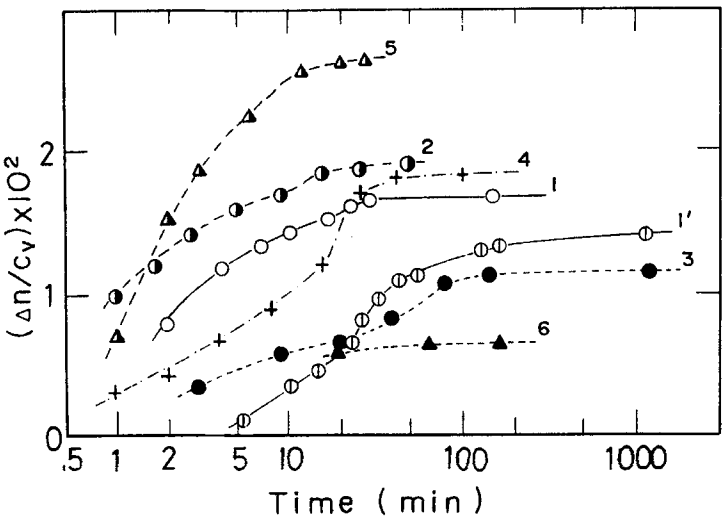

FIGURE 2 Change of the birefringence after the application of a magnetic field (2.5T). Lines, 1 and 1', PBLG (r = 470) in CH_2Br_2; 2, PBLG in CH_2Cl_2; 3, PBLG in dioxane; 4, an equimolar mixture of PBLG and PBDG (r = 530) in CH_2Br_2; 5, PELG ($r \cong 1{,}500$) in CH_2Cl_2; 6, PELG in dioxane. The polymer concentration was 14 vol% except for 1' (24 vol%).

dipole moment in the direction of the polymer helix. Because of the contribution of dipoles originated in the side-chains which point in the reverse direction, the magnitude of the dipole moment per residue turns to be 3.5 Debye in PBLG [30]. Any how PBLG thus tends to orient in the direction of electric field. The orientation of liquid crystals of PBLG in methylene bromide in low electric fields has been studied [27, 31]. In the dilute liquid-crystalline solutions of PBLG placed in an electric field, the polypeptide molecules behave as if independent molecular clusters having a permanent electric dipole moment of some 730 times as large as that of a single polypeptide molecule (of r = 650) were present in solution.

An electrically oriented PBLG film can be prepared by gradually drying up a liquid-crystalline solution in electric field applied parallel to the film surface. PBLG films so prepared was cut into strips perpendicular to the direction of orientation and rearragned to make a new film in which the molecular axis was roughly perpendicular to the surface of the film (new). The surface charge induced in this new film measured

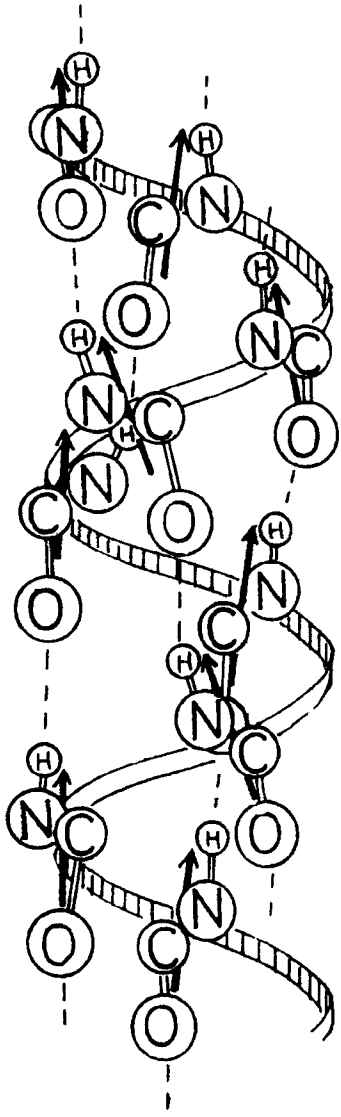

FIGURE 3 Orientation of the electric dipole moment, permanent, of the main-chain peptide group in an α-helical PBLG.

was $(60 \pm 20) \times 10^{-8}\,C/m^2$ [25], which was only some 0.6% of the amount of charge expected when assuming that all the permanent dipoles of the polypeptide molecules were in the same direction. This

implies that the polymer helices were distributed in molecular cluster with roughly equal likelihood in both directions to make most of the dipole moments (of the polymer helices) counterbalance each other. The electric-field orientation of PBLG is then considered to be induced by the excess of the dipole moments due to the fluctuation of the distribution of polymer molecules in the molecular cluster. The number, mean, of the polymer molecules in each molecular cluster, N, has been proposed to be given by $N^{1/2} = 730$ for PBLG (*of* $r = 650$) in methylene bromide. This results in $N = 5 \times 10^5$ [32, 33]. This value coincides in the order with that estimated for swarms of low-molecular weight liquid crystals [34].

To induce the magnetic-field orientation of a magnetically anisotropic particle, the potential energy of the particle in magnetic field should be larger than its thermal energy, that is

$$\mu B > kT \tag{11}$$

where μ is the magnitude of dipole moment of the particle, B is the magnetic induction. A single PBLG molecule will not fulfill the condition described by Eq. (6). PBLG molecules are expected to behave in the form of molecular clusters as in electric field.

Assuming the presence of molecular clusters and their three-dimensional Boltzmann distribution in solution, the order parameter has been derived as follows [29],

$$s = 1 - (3\coth x/x) + 3/x^2 \tag{12}$$

where x is substituted for $\mu B/kT$; When $x \ll 1$, the third term in this equation will be negligibly small. The birefringence, Δn, of a rigid molecule is expressed in the form [35],

$$\Delta n = 2\pi(g_1 - g_2)s/n \tag{13}$$

where $g_1 - g_2$ is the optical anisotropy factor and n is the refractive index in the absence of magnetic field. The following equation will be led accordingly,

$$\Delta n/c_v = [2\pi(g_2 - g_3)/n](1 - 3kT/\mu B) \tag{14}$$

(b) Order in Oriented Films

Highly oriented polypeptide films can be obtained in a magnetic field, applied parallel to the film surface, by drying the liquid-crystalline solution up slowly after the steady-state orientation is reached. X-ray diffraction photogaphs of a magnetically oriented PBLG film taken from three directions against the applied magnetic field clearly indicate double orientation [36, 37] of the α-helical molecules of PBLG with its fiber axis in the direction of the magnetic field as may be seen in Figure 4. The molecular axis of PBLG is parallel to the film surface. The uniplanar orientation of the PBLG molecules in the plane of the film occurs in the absence of magnetic field as well [38].

Under crossed nicols, magnetically oriented films of polypeptides show a striped pattern running perpendicular to the direction of the magnetic field (the direction of orientation) [36, 39]. A similar pattern is observed also in mechanically [40] and electrically [28] oriented films of polypeptides with respect to the direction of orientation. Magnetically oriented films of polypeptides have lamellar structures of thickness a few to several microns with their lamellae perpendicular to the field direction, and these lamellae are made up of rods (or sheets) of a diameter (or width) of about 0.1 μm aligning perpendicular to the lamellae (and parallel to the field direction) as may be seen in Figure 5; gap regions between the lamellae as observed in the electron micrographs are detected by the polarizing micrograph as the difference in the retardation.

The presence of rods (or sheets) can be seen also in the film cast and dried in the absence of magnetic field although the direction of

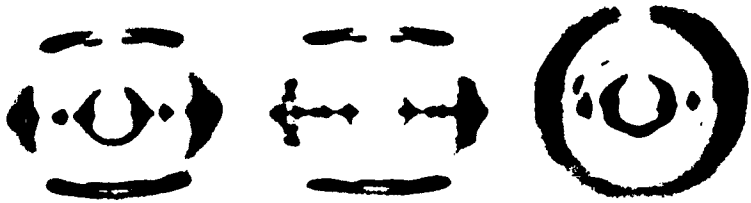

FIGURE 4 X-ray diffraction photographs of a magnetically oriented film of PBLG ($r = 650$). Cast and dried from methylene bromide solution in the magnetic field of 0.96 T. Beam normal to film (left), parallel to surface of film (middle), both direction of magnetic field vertical, and along the direction of magnetic field, the polymer film being in a vertical plane (right). (By courtesy of Mr. S. Ejiri).

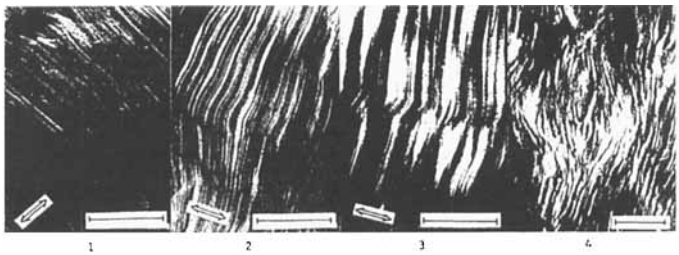

FIGURE 5 Electron micrographs of magnetically (and electrically) oriented films of polypeptides. 1. PBLG (r = 470), 0.75 T; 2. an equimolar mixture of PBLG (r = 470) and PBDG (r = 530), 2.5 T; 3. PBLG (r = 1,460), 180 V/cm; 4. same as in 2, no field. Cast and dried from methylene bromide solutions except 3 (methylene chloride solution). Bar, 5 μm; the arrows indicate the direction of external field.

orientation is random (Fig. 5). This agrees with the interpretation, based on observations of the small-angle light scattering by Wilkes [41], that the texture of unoriented films of PBLG is composed of randomly oriented anisotropic rods which are composed of oriented aggregates of the polymer molecules. These observations will be a strong indication for the presence of molecular cluster whose size is

"a few microns or more × 0.1 μϕ"

This size is suitable to accommodate 5×10^5 PBLG molecules (of r = 650). The size of rod varies depending on the systems as appeared in this text.

In the molecular cluster, the polymer molecules align nearly parallel to the cluster axis forming itself a crystallite; the crystallites so formed are aligned in the direction of magnetic field. The scattering intensity I of the circular record of the equatorial X-ray diffraction, at the Bragg angle of 6.70° from the (1 1 0) lattice planes, is well expressed by the following relation (29),

$$I = I_0 \exp[x \cos 2\theta] \tag{15}$$

where x is chosen as 3.7 for the film of PBLG of r = 470 prepared under the magnetic field of 2.5 T. The scattering intensity at any θ is in proportion to the number of polymer molecules ordering in the θ-direction, the direction that the polymer axis (cluster axis) makes

with the applied field direction, since the polymer axis is parallel to the film surface as mentioned above. The induced dipole moment of the molecular cluster is $\mu_0 \cos\theta$ (μ_0 is the dipole moment at $\theta = 0°$). The potential energy of the molecular cluster in the magnetic induction, B, has the magnitude $-(\mu_0 B/4)\cos 2\theta + \text{const}$. Therefore, the above relation indicates that the molecular clusters correspond to a two-dimensional Boltzman distribution in the plane of the film. The constant, x, can be interpreted to be substituted for $\mu_0 B/4kT$.

The degree of crystallite orientation Π can be expressed by the following equation [42],

$$\Pi = (90° - H°/2)/90° \tag{16}$$

where $H°$ is the half width read from the circular record of the intensity of the equatrorial diffraction corresponding the polymer-chain interval. The degree of the cluster (crystallite) orientation is then expressed as a function of x [28],

$$\Pi = 1 - [\cos^{-1}(1 - 0.6932/x)]/180° \tag{17}$$

By substituting the obtained data in this equation, the magnitude of the maximum induced dipole moment, μ_0 were calculated (Tab. I). The mean magnitude is about 2.4×10^{-17} erg/gauss for all the systems tested and any noticeable side-chain (of the polypepetide molecule) effect on the magnitude of the dipole moment could not be observed. The mean degree of orientation was 0.80 (or 80%). The maximum magnetic energy in a magnetic field of 1 T is then calculated to be about 0.15 eV (1 eV = 1.602×10^{-19} J). The number of PBLG molecules in molecular cluster was estimated to be about 5×10^5. So that, the magnetic energy per each peptide residue turns out to be about

TABLE I Maximum induced dipole moments of the molecular cluster and estimated birefringences of magnetically oriented film at complete orientation

Preparation	$\mu_0 \times 10^{17}$, *erg/gauss*	*Birefringence*
PBLG/CH_2Br_2	2.1 ~ 2.7	0.023
PBLG/dioxane	2.0 ~ 2.7	
1 : 1 PBLG-PBDG/CH_2Br_2	2.3 ~ 2.5	0.032
PELG/CH_2Cl_2	2.0 ~ 3.1	0.021

The values are the means of three specimens. (1 J/T = 10^3 erg/gauss).

TABLE II Percent fractional increase on swelling

Film	*N*	*X*	*Y*
No field	640	10	20
H//N	5	300	350
H//X	366	11	132

Films contained ~90% benzene by weight. PBLG (MW = 275,000) films cast in the magnetic field H of 1 T from a 12% solution in chloroform. N is the direction normal to the film surface, X and Y are axes in the plane of the film. (Reproduced from Samulski and Tobolsky [44]).

6×10^{-10} eV, which is about 1/100 of that estimated by Honda *et al.* [43]; the discrepancy has not been elucidated.

When cast with the magnetic field perpendicular to the film surface, there is competition between the uniplanar orientation and the orientation imposed by the magnetic field. Samulski and Tobolsky [44] have demonstrated that there are regions of high orientation where the molecular axis is tilted approximately 30° out of the film plane. They also have found unusual swelling properties of the cast film that depend on the condition of casting as may be seen in Table II. The swelling is reversible. The data in this table suggest that the swelling of the films results primarily from an increase in the lateral spacing between the molecules and translations in the direction parallel to the molecular axis are highly restricted. The normal α-helix contains 3.6 residues per turn. This α-helix is found in magnetically oriented nematic films of the isomer of PBLG when the film is cast from chloroform, whereas a distorted α-helix with 3.5 residues per turn is found in similarly prepared films cast from methylene chloride [45].

(c) Diamagnetic Anisotropy

According to Guha Sridhar *et al.* [46], the average susceptibility per molecule parallel and perpendicular to the nematic director (optic axis of an aligned nematic structure) $\sigma'_{\parallel}$ and $\sigma'_{\perp}$ are given by

$$\sigma'_{\parallel} = \sigma_{\text{iso}} + (2/3)(\sigma_{\parallel} - \sigma_{\perp})s,$$
$$\sigma'_{\perp} = \sigma_{\text{iso}} - (1/3)(\sigma_{\parallel} - \sigma_{\perp})s \tag{18}$$

where $\sigma_{\parallel}$ and $\sigma_{\perp}$ are the susceptibilities along and perpendicular to the longitudinal axis of the rod, $\sigma_{\text{iso}} = (1/3)(\sigma_{\parallel} + 2\ \sigma_{\perp})$ is the isotropic

susceptibility and s is the order parameter. Cylindrical symmetry for the rodlike helical polypeptide molecules are assumed. The molar diamagnetic anisotropy of a macroscopically aligned nematic $\Delta\chi'$ is then given by

$$\Delta\chi' = \chi'_{\parallel} - \chi'_{\perp} = N_A(\sigma'_{\parallel} - \sigma'_{\perp}) = (\chi_{\parallel} - \chi_{\perp})s \tag{19}$$

where $\chi'_{\parallel}$ and $\chi'_{\perp}$ are the susceptibilities parallel and perpendicular to the aligned nematic, respectively and N_A is Avogadro's number.

The magnetic-field orientation of polypeptides was first observed with PBLG and this was attributed in part to induced ring currents in the aromatic side chains of PBLG. In order to interpret the magnetic-field orientation of liquid crystals of this polypeptide, the idea that very large paramagnetic effects were produced by charge transfer with impurity oxygen atoms leading to holes in the benzene rings of the side chains of the polymer molecule was proposed [47].

Some time after this observation, polypeptides other than PBLG, such as poly (*L*-glutamic acid) [48], PELG [25, 49] and poly (*L*-lysine hydrobromide) [50], were shown to undergo the magnetic-field orientation. It is now believed that any polypeptide can orient in magnetic fields if only certain conditions are fulfilled. The magnetic-field orientation can be attributed to the diamagnetic anisotropy of the peptide groups, which are planar of the resonance between two valence-bond structure [51]:

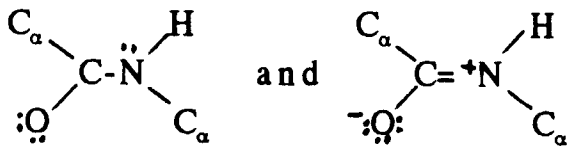

Pauling [52] has been able to lead the value of -5.36×10^{-6} CGS emu for the molar diamagnetic anisotropy of the peptide group according to a theory of the diamagnetic anisotropy of noncyclic planar groups of atoms with resonance structure (mobile electrons). The direction of the diamagnetic dipole induced in the peptide group is perpendicular to its plane. In the α-helical state, the peptide groups of a polypeptide molecule distribute with equal probability around the polymer axis and with their planes parallel to it. The polypeptide

molecule placed in a magnetic field is thus forced to align parallel and the planes of the peptide groups also parallel to the magnetic field in order to minimize the potential energy of the molecule.

The helicoidal axes of the cholesteric structure of liquid-crystalline solution of polypeptide tend to be perpendicular rather than parallel to the direction of applied magnetic field although only very small part of the polymer molecules satisfy the above-mentioned conditon. (When it is parallel, all the polymer molecules have the maximum potential energy.) The solution then becomes anisotropic and the torque exerts on such anisotropic solution when the direction of the magnetic field is altered. Using a torque magnetometer, Tohyama and Miyata [53] have been able to measure the anisotropy of diamagnetic susceptibility of PELG as $\Delta\chi = \chi_{\parallel} - \chi_{\perp} = (1.64 \pm 0.15) \times 10^{-8}$ emu/g at 30°C using a 20-wt% solution in ethyl acetate. This value is equivalent to -5.2×10^{-6} CGS/mol and agrees very well with that calculated by Pauling [52].

The anisotropy of diamagnetic susceptibility has been measured also using oriented films [54]. The anisotropy energy density ρ_e of the film is expressed as

$$\rho_e = (1/2)\Delta\chi' H^2 \sin^2\theta \tag{20}$$

where H is the field strength used in the torque measurement and θ, an angle between the field and the molecular orientation direction. The observed torque τ is given by

$$\tau = -(\partial E/\partial\theta) \cdot m \tag{21}$$

where m is the mass of the film. Using Eqs. (15) and (16), it is found that $\Delta\chi' = 1.18 \times 10^{-8}$ emu/g for PBLG. Taking into account of the distribution of the molecular axies of PBLG, $\Delta\chi$ ($= \chi_{\parallel} - \chi_{\perp}$) of PBLG is calculated as 4.52×10^{-8} emu/g.

Measured magnetic susceptibilities of polypeptides such as PBLG, poly (γ-ethyl *D*-glutamate) (PEDG) and poly (γ-methyl *L*-glutamate) (PMLG) in solid state are in good agreement with those calculated using Pascal's additivity rule [46, 55]. PEDG is an antipode of PELG and is expected to have the same susceptibility as that of PELG. The measured anisotropy of PELG is about 3% of the calculated susceptibility for PEDG, -0.54×10^{-6} emu/g. PELG (and PEDG) has no

magnetically anisotropic radical such as the phenyl group of PBLG. Thus the origin of the anisotropy will be only in the π-electrons of the peptide groups in the main chain of this molecule.

(d) Cholesteric-to-Nematic Transition

Electric and magnetic fields acting on the anisotropy of the electric or magnetic susceptibility exert torques within a liquid crystal which may compete with the elastic torques determining its internal structure. Meyer [56] derived equations describing the liquid crystalline structure with molecularly uniaxial liquid crystals on the basis of Frank's "curvature-elasticity theory" [57]. In doing so, the structure was determined so as to minimize the total free energy of the system, and this method was applied to the cholesteric structure.

According to Meyer [56], the pitch of the twisted structure increases with increasing strength of the applied magnetic field when the field direction is parallel to the molecular layers of the twisted structure. The amount of the increase, $P_{\|} - P_0$ is in proportion to F^4 to the lowest approximation where F is the field strength;

$$P_{\|} = P_0[1 + (\chi_{\|} - \chi_{\perp})]^2 F^4 P_0^4 / 32(2\pi)^4 k_{22}^2 \tag{22}$$

where k_{22} is the "twist elastic constant".

With visible light from a He-Ne gas laser (wavelength, $\lambda = 632.8$ nm) perpendicular to the magnetic field (and parallel to the molecular layers of the cholesteric structure), light diffraction patterns of the cholesteric solution are projected onto a ground glass plate in accordance with the Bragg equation due to the very large periodicities of transmittance of light [4],

$$n\lambda = P \cdot \sin\theta \tag{23}$$

where n is the order of reflection, $P/2$ is the distance between the planes at which reflections occurs (half pitch of the twisted structure) and θ is the angle between the planes and the direction of the incident light. The field strength dependence of the cholesteric pitch can be measured using this equation.

de Gennes [58] predicts an increase in the pitch, as the strength of an applied field is increased, with a logarithmic divergence of the pitch when the field strength approaches a critical value H_c

$$H_c = \pi^2[k_{22}/(\chi_{\parallel} - \chi_{\perp})]^{1/2}/2P_0 \tag{24}$$

This behavior is verified for thermotropic liquid crystals of low-molecular weight substances. Duke and DuPre [59] have shown that de Gennes' theory applies equally well to the lyotropic liquid crystals of polypeptides such as PBLG in dichloromethane.

When the field direction is perpendicular to the molecular layers of the twisted structure, the perturbation of the helical structure involves both bending and torsional strains, and depends on the relative magnitudes of the moduli of these strains, k_{33} and k_{22}, respectively [56]. If $k_{33} \geq k_{22}$, there is no perturbation until the critical field F_c is reached at which complete break down occurs; the pitch becomes infinity to form a nematic liquid crystal structure.

$$F_c = (2\pi/P_0)[k_{22}/(\chi_{\parallel} - \chi_{\perp})]^{1/2} \tag{25}$$

For $k_{33} < k_{22}$, no perturbation is caused until the magnetic field reaches $(k_{33}/k_{22})F_c$. Above this field strength, the pitch decreases in the following way

$$P_{\perp} = (k_{33}/k_{22})^{1/2}(F_c/F)P_0 \tag{26}$$

At $F = (k_{22}/k_{33})^{1/2}F_c$, however, there is a complete break down of the twisted structure leading to the cholesteric-to-nematic transition.

The ratio, $k_{22}/(\chi_{\parallel} - \chi_{\perp})$ can be determined from the slope of the line in the "$P_{\parallel} - P_0$ *vs.* F^4 plot" or by directly observing the break down of the twisted structure under the stage of a miroscope and using the equation for H_c. Then the observed value of $\chi_{\parallel} - \chi_{\perp}$ yields the twist elastic constant k_{22}. Toriumi *et al.* [60] have measured cholesteric-to-nematic transition parameters of PBLG liquid crystals in *m*-cresol using materials of various molecular weight at several polymer concentrations. The solvent used is known as a typical "aggregation free" solvent for PBLG especially in dilute solution [61]. Their results are shown in Table III.

TABLE III Cholesteric-to-nematic transition parameters in PBLG liquid crystals in *m*-cresol

MW	*Concn.* (*vol%*)	P_0 (μm)	$H_c(T)$	$k_{22}/\Delta\chi$ (*emu cgs*)	k_{22} (*dyne*)
9.5×10^4	15.0	35.5	0.75	29	2.0×10^{-7}
14.4×10^4	15.0	43.2	0.63	30	2.1×10^{-7}
24.6×10^4	15.0	53.8	0.53	33	2.3×10^{-7}
24.6×10^4	17.5	37.6	0.57	19	1.3×10^{-7}
24.6×10^4	20.0	27.8	0.63	13	9.1×10^{-8}
$*24.6 \times 10^4$	20.0	36.1	1.17	73	–

*Measured at 30°C (*83°C). $\Delta\chi$ was assumed to be 0.70×10^{-8} emu/cm^3 (1 JT^{-2}m^{-3} = 10^{-7} emu/cm^3) according to DuPre and Duke [63] (1 SI unit for $k_{22}/\Delta\chi$ is 10^8 emu cgs and 1 N = 10^5 dyne. Prepared after Toriumi *et al.* [60]).

Straley [62] has claimed that k_{22} is proportional to the fourth power of the helix length L,

$$k_{22} = c \cdot C^2 L^4 D \cdot kT \tag{27}$$

where c is a constant ($c \cong 0.02$), C is the molecular concentration in vol%, D is the helix diameter, and kT has its usual meaning. The helix length increases by 1.5 Å every additional residue. They have been unable to confirm the strong molecular weight dependence of k_{22} as predicted by Eq. (22). Du Prè and Duke [63] reported a value of 6.2×10^{-8} dyne (1 N = 10^5 dyne) for a MW 31×10^4 PBLG in dioxane and Guha Sridhar *et al.* [46], a value of 582×10^{-8} dyne for MW 55×10^4 PBLG in methylene chloride. Therefore, the value of k_{22} appears to depend on the solvent used.

The value of H_c decreases with increasing molecular weight inversely proportional to P_0 as predicted by Eq. (19). The value of P_0 decreases with increasing C value; however, the value of H_c increases only slightly. The value of k_{22} decreases with increasing C value, which is against the prediction given by Eq. (19). The sense of cholesteric phase turns to left-handed from right-handed at 60°C. The values of H_c and $k_{22}/\Delta\chi$ show a drastic decrease accordingly. Since both k_{22} and $\Delta\chi$ are known to decrease in magnitude with temperature [64], they have concluded that the reduction of $\Delta\chi$ value exceeds that of k_{22} value.

Guha Sridhar *et al.* [46] have also measured the rotational viscosity coefficient η of the PBLG liquid crystal in methylene chloride by observing the reorientation of the nematic director in a magnetic field.

When the sample axis (orientation of the nematic director) is quickly rotated by 90°, the magnetic moment changes with the characteristic reorientation time t_R,

$$t_R = \gamma_1/(\Delta\chi)H^2 \tag{28}$$

Assuming that $\Delta\chi = (7.0 \pm 0.7) \times 10^{-6}$ emu/mole, they have obtained the coefficient $\eta = 2.8 \times 10^5$ P (1 Pa · s = 10 P).

3.2. Polyribonucleotides and DNA

(a) Nematic Mesophase

Double-stranded helices of poly (A + U), poly (G + C) and poly (C + I), and triple-stranded helices of poly (A + 2U) and poly (A + 2I) in concentrated solution form nematic liquid crystals. The molecular assemblies of the two complexes of poly (A) and poly (U) are rod-like and align themselves with their long axes parallel to the direction of orientation. On standing for several weeks liquid crystals of these two complexes are converted from the nematic to the cholesteric type as shown in Figure 6, which reverses to the nematic phase, oriented, under shearing stress [65].

Films of those two complexes cast from their nematic solutions under a magnetic field of 2.5 T (The magnetic field is parallel to the surface of the films.) show X-ray diffraction patterns having two equatorial spacing at 3.3 Å and 3.8 Å, and two meridian spacings at 4.6 Å and 5.8 Å when the direction of magnetic field is vertical as may be seen in Figure 7. The 3.3 Å spacing is related to the stacked bases whose plane is nearly perpendicular to the helical axis [66]. Thus, the X-ray results suggest that these polymer complexes are oriented in the direction perpendicular to the magnetic field in accordance with the suggeston by Maret *et al.* [10]. The diamagnetic dipole is expected to be induced in the base due to the benzene-like molecular orbital above and below the plane of the ring [67]. Since the plane of the base rings is roughly perpendicular to the helical axis in these complexes, the direction of the induced diamagnetic dipole is perpendicular to the plane and parallel to the polymer helix. This is consistent with the observed direction of magnetic-field orientation of the polyribonucleotide complexes.

FIGURE 6 Polarizing micrographs of liquid crystals of poly (A + U). Left, nematic phase; right, cholesteric phase.

The liquid-crystalline solutions of poly (A + U) and poly (A + 2U) show the small-angle light scattering H_v pattern of the $\pm 45°$ type, suggesting the presence of a collection of rod-like assemblies of the polymer helices (molecular clusters) with maximum polarizability in the direction either parallel or perpendicular to the rod axes [39, 68]. When the liquid crystalline solution is sheared vertically in an optical

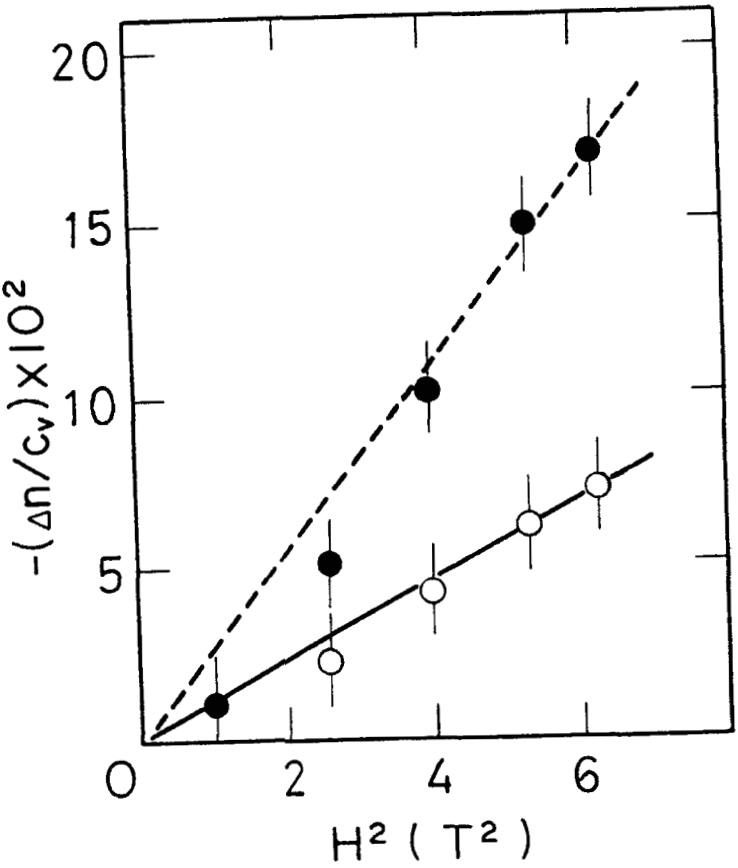

FIGURE 7 X-ray diffraction photographs of a magnetically oriented film of poly (A + 2U). The field strength was 2.5 T and the direction of magnetic field vertical. See the caption to Figure 4.

cell by moving a spacer up and down inside the cell, the upper (and lower) angles of intersection of the cross pattern ($\pm 45°$ type) become larger than 90° [39]. Thus, the molecular clusters align themselves with their long axes parallel to the direction of shearing stress. At the absorption band near 260 nm the oriented polyribonucleotide complexes in solution shows a larger absorbance when the electric vector of the incident beam is perpendicular to the shear direction than when it is parallel. This band is related to the $\pi - \pi^*$ transition in the purine and pyrimidine bases of the nucleotides and the direction of this

transition moment is in the planes of these base rings [69]. Therefore, this linear dichroism results indicate that the helical complexes align themselves parallel to the rod axis of the molecular cluster.

The torque τ acting on the rodlike molecular cluster in a magnetic field H will be given by the following equation [70],

$$\tau = |\mathbf{M}_{\parallel} \times \mathbf{H} - \mathbf{M}_{\perp} \times \mathbf{H}| = (1/2)(|\chi_{\parallel}| - |\chi_{\perp}|)H^2 \cdot v \cdot \sin 2\theta \qquad (29)$$

where $\mathbf{M}_{\parallel}$ and $\mathbf{M}_{\perp}$ are the components of a magnetic dipole induced in the molecular cluster, respectively parallel and perpendicular to the long cluster axis, $\chi_{\parallel}$ and $\chi_{\perp}$ are magnetic susceptibilities corresponding to $\mathbf{M}_{\parallel}$ and $\mathbf{M}_{\perp}$, respectively, θ is the angle that the long cluster axis makes with the direction of magnetic field and v is the volume of molecular cluster (Fig. 8). The potential energy of the molecular cluster, U, at any θ will be given in a form,

$$U = -\int \tau d\theta = (1/4)\Delta\chi \cdot H^2 \cdot v \cdot \cos 2\theta, \quad \Delta\chi = |\chi_{\parallel}| - |\chi_{\perp}| \qquad (30)$$

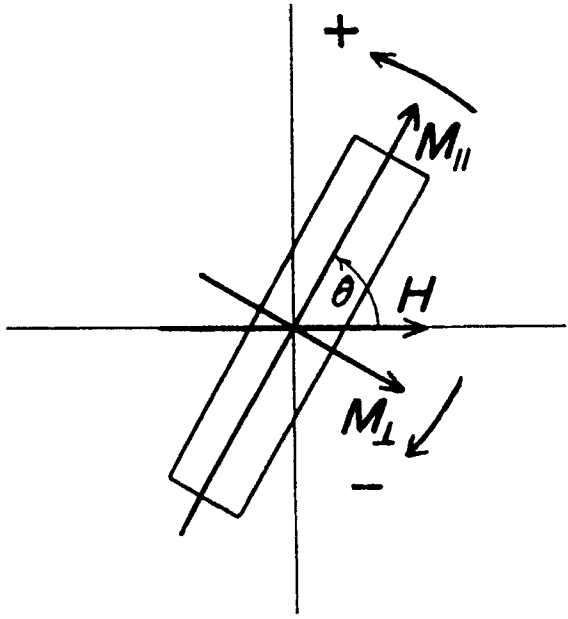

FIGURE 8 Orientation of a diamagnetic rod in a static magnetic field.

If $|\chi_{\parallel}| > |\chi_{\perp}|$, the potential energy becomes minimum at $\theta = 90°$, which explains the way of arrangement of the helical complexes of polyribonucleotides in magnetically oriented polymer films. The upper (and lower) angles of intersection of the cross H_v pattern becomes larger than 90° when the magnetic field is applied to the solution horizontally. This indicates that the long axis of the molecular cluster (and the helical axis of polyribonucleotides) is perpendicular to the magnetic field as expected.

Since the polyribonucleotide helices have negative birefringence [71], the refractive index of a magnetically oriented nematic solutions is larger for light whose electric vector is parallel than perpendicular to the direction of magnetic field (and to the direction normal to the axes of polyribonucleotide helices). The nematic solution of polyribonucleotide complexes in magnetic field will be assumed to be a system of rods having induced, magnetic dipole moments. The order parameter s of this system is given in the form [72],

$$s = (1/2)\int_0^{\frac{\pi}{2}} (3\cos^2\theta - 1)\exp(-U/kT)d\Omega \Big/ \int_0^{\frac{\pi}{2}} \exp(-U/kT)d\Omega \quad (31)$$

where θ is the tilt angle of rod axis with respect to the position of energy minimum. U is the potential energy of rod in a static magnetic field H and is given by replacing θ with $(\pi/2) - \theta$ in Eq. (25). Substituting x for $\Delta\chi \cdot v \cdot H^2/4kT$ and y for $\cos\theta$ and approximating the exponential function as $1 + x(2y^2 - 1)$ provided that $x \ll 1$, the following result is obtained [70],

$$s = 0.067\Delta\chi \cdot v \cdot H^2/kT \quad (32)$$

This result predicts that the value of s is proportional to the square of magnetic field strength and is consistent with the experimental result except at field strengths lower than about 1.6 T as may be seen in Figure 9. It should be noticed that s was calculated with respect to the rod axes which are perpendicular to the "long" rod axes. Considereing the random orientation of rods around the axis parallel to the direction of magnetic field, the birefringence $\Delta n/c_v$ of the system will be given by

$$\Delta n/c_v = (1/2)(\Delta n/c_v)_0 s \quad (33)$$

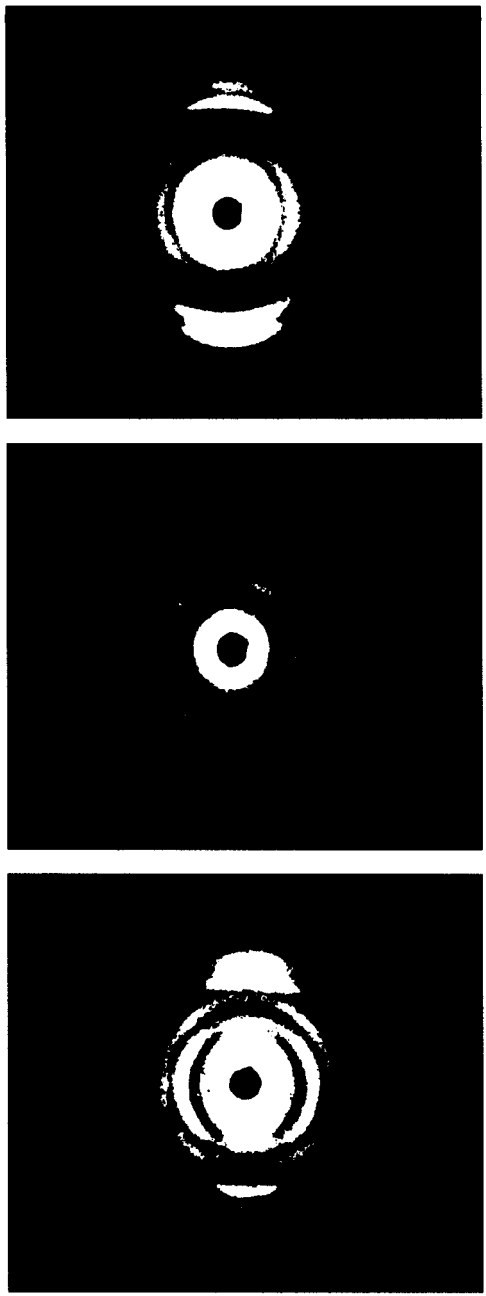

FIGURE 9 Values of the steady-state birefringence as a function of the square of magnetic-field strength. Full line, poly (A + U) – 8.1 vol% and broken line, poly (A + 2U) – 10.5 vol%.

where c_v is the volume fraction of rods, and $(\Delta n/c_v)_0$ is the birefringence at perfect orientation and is about 0.1 [71].

Measurements of the birefringence of liquid-crystalline solutions were carried out in a quartz cell of path length 1 mm with a quartz spacer to reduce the path length. The decay of birefringence of the oriented nematic solution of poly (A + U) or of poly (A + 2U) after removal of the external magnetic field (of 2.5 T) is well expressed by the sum of two exponential components [70],

$$\Delta n/c_v = (\Delta n/c_v)_{t=0}[C\exp(-t/t_1^*) + (1-C)\exp(-t/t_2^*)] \qquad (34)$$

where t_1^* and t_2^* are relaxation times and C is a constant having a value between 0 and 1. Examples of the numerical results are shown in Table IV. The first term in Eq. (29) decays more than 5 times faster than the second and is considered to be related to some wall effects by which the rodlike molecular clusters are forced to be rearranged in some specific manner with respect to the interior surface of the optical cell and to the surface of the spacer inserted. Judging from the values of C and solution thickness, the limit of range (coherent length) in which the rodlike molecular clusters are under the influence of walls is estimated to be about 10 μm from the wall. The second term is considered to be free from the wall effects, to which the deviation of the steady-state birefringence from the predicted value (Fig. 9) will be related. The value of apparent rotational diffusion constant Θ of the rodlike molecular cluster, as calculated using the relation, $\Theta = (1/6)t_2^*$, has the order of $10^{-4}\,\mathrm{sec}^{-1}$.

TABLE IV Decay of the birefringence of magnetically oriented solutions after removal of the magnetic field

Preparation	*Concn.* (*vol*%)	t_1^* (*sec*)	t_2^* (*sec*)	Θ ($\times 10^{-4}$ *sec*$^{-1}$)	C	*Thickness* (*μm*)
Poly (A + U)	8.1	140	770	2.16	0.45	98
	10.5	135	2530	0.66	0.51	33
Poly (A + 2U)	8.1	205	1030	1.62	0.38	58
	10.5	190	1010	1.65	0.40	58

The measurements were carried out at 20°C.

TABLE V Tentative values of $k_{22}/(\chi_{\parallel} - \chi_{\perp})$

Preparation	*Concn. (vol%)*	$k_{22}/(\chi_{\parallel} - \chi_{\perp})$ *(emu cgs)*
Poly (A + U)	8.1	1.6
	10.5	1.3
	12.8	1.4
Poly (A + 2U)	10.5	6.0
	14.5	3.4

(b) Cholesteric Mesophase

The cholesteric pitch of the two complexes of poly (A) and poly (U) increases when the strength of a magnetic field applied parallel to the molecular layers of the twisted structure is increased. The amount of increase $P_{\parallel} - P_0$ is in proportion to F^4 as in the case of the cholesteric liquid crystal of polypeptides [73]. Although the relationship is not perfectly linear unlike in the latter case, values of $k_{22}/(\chi_{\parallel} - \chi_{\perp})$ can be determined from the slope of the line in "$P_{\parallel} - P_0$ *vs.* F^4 plot" and are shown in Table V.

4. THERMOTROPIC LIQUID CRYSTALS

4.1. Polyesters

There are two approaches to prepare thermotropic liquid-crystalline polymers: one approach is to incorporate mesogenic or rigid groups into a flexible polymer backbone [8, 74] and the other, to attach these groups to a flexible main chain as pendant groups (comb-like polymers) [75, 76]. Polymers comprising alternate linkage of mesogenic element and flexible spacer group such as

$$(CH_2)_n, \quad (CH_2\text{-}CH_2\text{-}O)_n, \quad \text{or} \quad \left(\begin{array}{c} CH_3 \\ | \\ Si\text{-}O \\ | \\ CH_3 \end{array}\right)_n$$

can give thermotropic mesophases in which the transition temperatures are well below the range of thermal degradation of the

macromolecule [77]. A polymer synthesized by Volino *et al.* and called DDA9-L [78] is one of the first examples among various thermotropic liquid crystalline polymers of this kind,

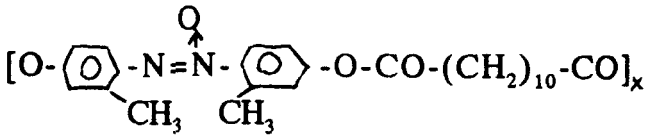

The average molecular weight of this polymer is 7,000 which corresponds to an average degree of polymerization of 15, and the nematic phase extends from 98 to 185° between the solid and the isotropic phases.

According to Volino *et al.* [78], the proton NMR spectrum of DDA9-L in the magnetic field of 1.17 T is a simple broad line between room temperature and 70°. Between 70° and the solid-to-nematic transition, two shoulders, distant of $2\delta i$, appear in the spectrum. At the solid-to-nematic transition, the spectrum suddenly broadens and becomes better resolved. A well defined doublet $2\Delta_N$ such that $2\Delta_N \approx 4\delta_i$ appears at the same time and the splitting $2\Delta_N$ decreases as the temperature increases in a manner which resembles that of a nematic order parameter. From these experimental evidences they have claimed that the spectrum transforms from a "powder" spectrum to an "aligned" spectrum along the magnetic field and consequently, that an alignment of the molecules occurs at the transiton. The splitting $2\Delta_N$ at 120°C is about 20 kHz (4.7 gauss, or 4.7×10^{-4} T).

Volino *et al.* [78] have suggested by comparing the shape of the spectra at 92° and at 120° (before and after the transition) that not only the mesogenic groups but also the flexible groups are aligned in the magnetic field. This result agrees well with the model proposed for the structure of a similar nematic polymer, on the basis of X-ray diffraction results [79]. They have approximately simulated the NMR spectrum of the protons of the mesogenic groups of DDA9-L, at 120°C, for the two most probable configurations, *i.e.*, with the methyl groups, either on the same side, or in opposite side. It has been shown further that the configuration where the two methyl groups are on the same side, and where the two phenyl rings form a certain dihedral

angle, are the most likely. The order parameter s varies from ~ 0.88 to ~ 0.72 over the whole nematic range.

Hardouin *et al.* [80] have made magnetic measurements on a series of polyesters in their nematic state and compared to their apparent viscosity at the same temperature. In accordance with de Gennes's theory [81], the main chain of these liquid crystalline polymers is constituted of alternating mesogenic moieties and flexible segments,

where n characterizes the flexible chain ($5 \leq n \leq 12$). These polyesters, designated C_n, exhibit a wide stable mesomorphic range below the decomposition temperature. All the number-average molecular weights are about 10,000 (x being about 25) except for one of the two C_5s. Except the C_5 in question, the apparent viscosity coefficient measured at the lowest rotational velocity (1 rpm), which represents the experimental value colsest to η_0 (at 0 rpm), increases in the order, C_6, C_5, C_8, C_7, C_9 and C_{12} starting from 1,635 cP (1 Pa · s = 10 P = 10^3 cP) up to 33,290 cP. Only the polymer C_6 shows two constant limiting Newtonian viscosities η_0 and η_∞, respectively, for low and high shear rates (between 1 – 256 rpm and at 210°C).

These polyesters show a fluid anisotropic phase of the nematic type and a magnetically orienting behavior in the mesophase range. A sample (mass m) located in a magnetic induction gradient $B \cdot (\partial B/\partial x)$ (where x is the distance of the sample from the polar axis) generates a magnetic force F which is related to the magnetic susceptibility χ per unit mass by the following equation [82],

$$F = (1/2\mu_0)(\partial B^2/\partial x)\chi m. \tag{35}$$

Hardouin *et al.* [80] have measured this force with a microbalance and consequently the magnetic susceptibility. According to Noel *et al.* [83], the apparent magnetic anisotropy $\Delta\chi'$ is given by

$$\Delta\chi' = (3/2)(\chi_{\parallel H} - \bar{\chi}) \tag{36}$$

where $\chi_{\parallel H}$ is the magnetic susceptibility parallel to the magnetic field and $\bar{\chi}$ the average susceptibility determined on powdered samples at room temperature. The extent of the orientation is thus characterized

by $\Delta\chi$. Hardouin *et al.* [80] first observed the tendency of these polymers to become aligned spontaneously in the bulk as a function of the magnetic field strength (0–1.5 T) and measured the magnetic susceptibility $\chi_{\|H}$ for increasing magnetic field strength to calculate values of $\Delta\chi'$.

According to them, the minimum magnetic field strength needed to induce spontaneous orientation and sufficient time needed to reach the saturated values of $\Delta\chi'$ at 1.5 T increase with increasing viscosity of the sample. The former varies from 0.4 T to 1.3 T and the latter from 0 to 190 min (C_{12} does not show magnetic-field effects.). The values of $\Delta\chi'_{max}$ decreases with increasing viscosity of the sample starting from 1.10×10^{-7} emu cgs g^{-1} ($1\,JT^{-2}\,kg^{-1} = 10^{-4}$ emu cgs g^{-1}) (C_5) to 0.48×10^{-7} emu cgs g^{-1} (C_9) and it becomes zero in C_{12}. Thus, with a molecular weight of same order of magnitude, the length of the flexible segment of the main-chain polymers plays an important role in the magnetic orientation effects. The value of 1.1×10^{-7} emu cgs g^{-1} corresponds to the diamagnetic anisotropy usually obtained for low-molecular weight liquid crystals in the nematic phase [84]. On cooling from the oriented nematic phase (at 210°C) in the magnetic field, the alignment is maintained down to room temperature.

4.2. Polypeptides

So far, any comb-like polymers reported have included polyhydrocarbon or polysiloxane, $H_3SiO\text{-}(H_2SiO)_n\text{-}SiH_3$, in the main chain. Kasuya *et al.* [85] synthesized copoly (γ-*n*-alkyl *L*-glutamate)s that assumed the cholesteric mesophase when two different alkyl groups were combined in a ratio of about 50/50 mol% and the preparations were annealed at 110–190°C. Hanabusa *et al.* [86] synthesized derivatives of PBLG having long alkyl side-chains as pendant groups. These polymers were the first to show that polypeptides can also form thermotropic liquid crystals. These thermotropic polypeptides all consist of a mesogenic or rigid backbone and flexible side-chains as pendant groups. They are similar in architecture to comb-like polymers; however, they differ from genuine comb-like polymers in the point that the latter have a flexible backbone and rigid side-chains.

Poly(*L*-glutamate) esters with long alkyl side-chains containing a mesogenic aromatic segment at the terminal position shows below are

α-helical [87].

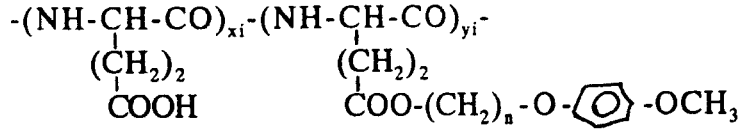

The degree of polymerization, $\Sigma x_i + \Sigma y_i$, of the polymer with $n = 6$ (designated R6) was 940 and the degree of substitution was 98%. This specimen undergoes the crystal-to-liquid crystal transition at about 27°C where the side-chains melt and act as a solvent for the rigid main chain [88]. When in a capillary tube of the inside diameter 1 mm, the polymer helices exhibit spontaneous orientation in the direction of the axis of the tube at 160°C. Arrangement of the polymer helices in the capillary tube is rectangular and turns to hexagonal when cooled to room temperature where the polymer helices are in the solid (crystalline) state. The rectangular unit cell has dimensions, $a = 45.12$ Å and $b = 13.16$ Å in the cross section, and includes two polymer chains.

When in liquid-crystalline state (at 160°C), R6 becomes oriented in a magnetic field (0.6 T) although the orientation is not good unlike in the case of PBLG [89]. On cooling from the oriented nematic phase, the orientation is maintained down to room temperature. Measurements of the X-ray diffraction pattern has shown that the arrangement of the polymer helices is perpendicular to the field direction unlike in PBLG. This suggests that there is some driving force which overcomes that of the peptide groups to arrange the polymer helices in the field direction. The anisotropy of diamagnetic susceptibility of the benzene groups of this polymer is a candidate for this driving force.

A small amount of R6 was put on a calcium fluoride plate and was spread in one direction with a spatula and a forefinger cushion to make an oriented polymer film in which the polymer helices were in the direction of spreading. The infrared dichroism of the oriented films so prepared was analyzed [88]. According to Tsuboi [26], two transition moments, the Phenyl A_1 centered at 1,453 cm^{-1} and Phenyl B_1 centered at 1,501 cm^{-1} are both in the plane of benzene ring and perpendicular with each other. This should be the case also in R6. Both two Phenyl transition moments has shown the perpendicular dichroism though weak, suggesting that the planes of the benzene rings, which are

distributed around the polymer helix at an equal probability, are perpendicular rather than parallel to the polymer axis, whereas the planes of the peptide groups are parallel to it.

The induced diamagnetic moment (maximum) μ of a benzene ring is given by Pople [90] in the form,

$$\mu = 3e^2Ha/2\pi mc^2 \tag{37}$$

where a is the area of the benzene plane and is roughly πd^2 (d being the C—C distance), e and c have their usual meanings and Gaussian system of units being used. The value of μ is then calculated at 1.2×10^{-28} emu/gauss (1 J/T = 10^3 emu/gauss). The observed anisotropy of magnetic susceptibility of PELG which lacks benzene groups is 1.64×10^{-8} emu/g [53]. This magnetic susceptibility arises from the peptide groups of this polymer. The anisotropy of magnetic susceptibility is equal to the magnetic dipole moment per unit volume and per unit field strength. Diving this value by the number of peptide group in 1 gram of PELG, the induced magnetic dipole moment due to one peptide group is estimated to be 4.6×10^{-30} emu/gauss [89]. Therefore, the induced diamagnetic dipole moment of the benzene group which points to the direction parallel to the polymer helix is larger by about 25 times than that of the peptide group which points to the direction perpendicular to the polymer helix. This would explain the reason why the polymer helices orient in the direction perpendicular to the external magnetic field. The orientation is brought about as the result of cooperative behavior of the polymer helices as in the lyotropic liquid crystals of PBLG.

In this connection, there is not much difference in observed magnetic susceptibility between PBLG and PELG which lacks benzene groups (Tab. III). This suggests that the planes of the benzene rings of PBLG which are distributed around the polymer helix at an equal probability roughly make the magic angle of 54°44′ so that the magnetic-field effect of benzene rings is counterbalanced if not completely.

5. LIVING SYSTEMS AND RELATED COMPOUNDS

Building blocks for living systems are cells which are small membrane-bound compartments filled with a colloidal solution of chemicals. All

biological membranes including the plasma membrane of eucaryotic cells, have a common overall structure as Alberts *et al.* [7] have suggested. They are assemblies of lipid and protein molecules held together by noncovalent interactions. Lipid molecules are arranged as a continuous double layer of 4–5 nm thick. This lipid bilayer bears a close resemblance to the smectic mesophase of liquid crystal. Liquid-crystal-like structure found in living systems, however, are not genuine liquid crystals like those of synthetic compounds, and often called "super mesophase" [91]. Liquid crystals allow for liquid-like diffusion and for the transition of energy and information in a selective manner over long distances. Besides, they respond to detection of heat, light, electric and magnetic fields, sound, mechanical pressure and chemical environment with high sensitivity [7]. The function of living systems is indebted to such a specific characteristic of liquid crystals. Various living systems have been found to be affected by a magnetic field.

5.1. Sickled Erythrocyte

A human erythrocyte holds a concentrated (about 30%) solution of hemoglobin in it. Deoxygenated sickle-cell hemoglobin (deoxy Hb S) in concentrated solution aggregates to form gels that are temperature dependent. This is believed to be the result of close ordering of deoxy Hb S into linear aggregates. Finch *et al.* [92] interpreted each aggregate as a tubular fiber made up of six thin strings of hemoglobin molecules linked end to end at intervals of 64 Å in wet fibers and each string was wound around the tubular surface with a helicoidal pitch of about 3,000 Å. The appearance of these fibers-as clusters of parallel rods-resembles descriptions of liquid crystals of the nematic type [93].

Deoxy Hb S has a paramagnetic moment of 5.35 Bohr magnetons (1 Bohr magneton = 0.927×10^{-23} J/T) per haem group [94] and the rodlike assemblies of this protein in which the plane of the haem groups is oriented essentially parallel to the rod axis is expected to have enough dipole moment to orient in magnetic field. Sickled erythrocytes whose long axes are prepfered directions for the deoxy Hb S fibers actually align with their long axes perpendicular to the direction of a magnetic field of 0.35 T when dispersed in solution [95]. However, cell-free liquid crystals of deoxy Hb S has not shown any magnetic-field effect even in a magnetic field of 2.5 T [96]. This may be due to the lack of fluidity of the liquid crystals.

5.2. Viruses

Torbet and Maret [97] have measured the birefringence of bacterial viruses Pfl and fd in dilute aqueous solution under magnetic fields up to 13.5 T. Pfl and fd are strains of rodlike single-stranded DNA containing bacteriophages with a diameter of 60 Å. The molecular weight and length are 37.5×10^6 and 19,600 Å for Pfl and 16.4×10^6 and 8,800 Å for fd. Pfl is composed of 7,600 major coat protein molecules and 7,400 nucleotides, whereas the numbers of these components are 2,700 and 6,400 in fd. In addition to these components, each virus contains certain other proteins. The Pfl major coat protein consists of 46 amino acid residues, of which 2 are aromatic, whereas in the fd coat protein these numbers are 50 and 6, respectively. The DNA is encapsulated in a helical shell of coat proteins [98].

The induced birefringence Δn in a magnetic field at right angles to the direction of the light ray is given by Eq. 2.4. Torbet and Maret [97] have been able to derive equations for the Cotton-Mouton constant C_M and the anisotropy of diamagnetic susceptibility $\Delta\chi$,

$$C_M = (2\pi/135)\left[(n_0^2 + 2)^2/n_0\right](1/\lambda kT)(cN_A/M_r)\Delta\chi\Delta\alpha \tag{38}$$

$$\Delta\chi = C_M 15\lambda kT/\Delta n_{sat} \tag{39}$$

where n_0 is the mean refractive index of the solution, c is the concentration of the solution (dilute), N_A is Avogadro's number, M_r is the molecular weight, and $\Delta\alpha$ is the anisotropy of optical polarizability. Shear-aligned solutions of fd fibers are positively birefringent with respect to the direction of shear stress [99]. The magnetic birefringence of both phages is positive, therefore, they are known to orient parallel to the direction of magnetic field. The axis of smallest numerical diamagnetic susceptibility is then parallel to the virus long axis and $\Delta\chi$ is positive. The specific Cotton-Mouton constant C_M/c is independent of concentration c, suggesting that interparticle interactions are weak under these conditions. It is $(1.97 \pm 0.1) \times 10^{-4}\,T^{-2}\,cm^2\,mg^{-1}$ ($1\,T^{-2}\,m^2\,kg^{-1} = 10^{-2}\,T^{-2}\,cm^2\,mg^{-1}$) for Pfl and is $(0.97 \pm 0.05) \times 10^{-4}\,T^{-2}\,cm^2\,mg^{-1}$ for fd [97].

No saturation of Δn is reached even in the highest magnetic field used when in dilute (isotropic) solution. Above a critical concentration (about 7 mg/ml for Pfl and about 10 mg/ml for fd), however, there is an abrupt transition to a solution and due to cooperative behavior of the

polymer molecules in liquid-crystalline state their full alignment can be attained. The average high-field saturation values of $\Delta n_{sat}/c$ are $6.27 \times 10^{-5}\,mg^{-1}\,ml$ ($1\,kg^{-1}l = 10^{-3}\,mg^{-1}\,ml$) for Pfl and $6.00 \times 10^{-5}\,mg^{-1}\,ml$ for fd. Thus, the value of $\Delta\chi$ can be determined from Eq. (2) as $1.22 \times 10^{-23}\,JT^{-2}$ for Pf and $0.63 \times 10^{-23}\,JT^{-2}$ for fd [97].

Both anisotropies, $\Delta\chi$ and $\Delta\alpha$, can have both a shape and intrinsic component. Assuming that the shape component especially in $\Delta\chi$ is negligible and that the major contributions to the intrinsic anisotropies come from the α-helices and aromatic amino acid residues of the major coat protein and from the DNA bases, Torbet and Maret [97] have shown that in both phages the α-helices and aromatic amino acids are oriented relatively parallel to the phage axis. In Pfl these become, on average, more nearly parallel as the temperature is reduced from about 25 to 5°C. They have been able to estimate that $\Delta\chi_a = -10.5 \times 10^{-28}\,JT^{-2}$ and that $\Delta\chi_D = -4.8 \times 10^{-28}\,JT^{-2}$ for Pfl and $-4.6 \times 10^{-28}\,JT^{-2}$ for fd assuming that $\Delta\chi_\alpha = 4.45 \times 10^{-29}\,JT^{-2}$ according to Pauling [51] where the subscripts a, D and α denote the aromatic residues, DNA bases and α-helices, respectively. In doing so, the number of each molecular group N_i was taken as $N_\alpha = 3.5 \times 10^5$, $N_a = 15{,}200$, $N_D = 7{,}400$ for Pfl and $N_\alpha = 1.35 \times 10^5$, $N_a = 16{,}200$, $N_D = 6{,}400$ for fd.

Tobacco mosaic virus (TMV) is another example undergoing the magnetic-field orientation [67]. TMV is a rodlike particle with a diameter of 15 nm. The molecular weight and length are 40×10^6 and 300 nm, respectively. It is composed of 2,200 coat protein molecules and 1 RNA molecule encapsulated in a helical shell of coat proteins as in Pfl and fd [100]. The coat protein is composed of 158 amino acid residues and have a molecular weight of 17,400. The molecular weight of RNA is about 2×10^6. This phage is partially aligned in the direction of a magnetic field of 0.9 T; the induced birefringence is 3.58×10^{-9} when the concentration of the solution is 2.44 mg/ml and the value of $\Delta\chi$ being $2.9 \times 10^{-24}\,JT^{-2}$ per phage. The magnetic-field orientation of TMV is concluded to originate in the α-helices of the coat proteins as in Pfl and fd.

5.3. Biological Membranes

Suspensions of various biological membranes such as retinal-rod outer segments [101], chloroplasts [102], and purple membranes from

Halobacterium halobium [103] are shown to orient in a magnetic field. In all these membrane systems, the plane of the membranes is arranged perpendicular to the field direction. Phospholipids, which are the major components of biological membranes, are thus oriented with their hydrocarbon chains parallel to the magnetic field. If the diamagnetic anisotropy of phospholipids with two long hydrocarbon chains is assumed to be similar to that reported for a long hydrocarbon-chain fatty acid such as steric acid [104], the membrane should orient parallel to the field instead of perpendicular. Thus the observed direction of magnetic-field orientation is in contradiction to what is expected from the assumed diamagnetic anisotropy of phospholipids. This is usually explained that the orientation effect results from the summed anisotropy of proteins in a membrane which is partially cancelled by that of phospholipids.

In order to give further convincing proofs of the role of phospholipids and proteins in the magnetic-field orientation of biological membranes, Sakurai *et al.* [103] and Kawamura *et al.* [105] have studied the diamagnetic anisotropy of single crystals of *L*- and *DL*-dipalmitoylphosphatidylcholine (DPPC) and of polyethylene (PE). These crystals are obtained from xylene suspensions as thin platelets. The *L*-DPPC crystal are rectangular and have rather uniform dimensions with one another. The average dimensions of the crystals they used are $36 \times 18 \times 0.1\ \mu m$.

In the platelet, DPPC molecules form a bilayer and PE molecules, a multi-layer structure. The plane of layered structure is parallel to that of the platelet and hydrocarbon chains are aligned nearly perpendicular to the plane of platelet. Those crystals suspended in xylene become oriented in the magnetic field of about 0.5 T in such a manner that the plane of the platelets are parallel, that is, the hydrocarbon chains are perpendicular to the filed direction; phosphorylcholine groups of DPPC's are also oriented in a similar way [105]. The orientation direction of hydrocarbon chains is consistent with the reported anisotropy of diamagnetic susceptibilities for long hydrocarbon chain compounds.

The orientational relaxation time t_R in a magnetic field is given in the form [106]:

$$t_R = \zeta/(\Delta\chi \cdot V \cdot H^2) \tag{40}$$

where ζ is the rotatory friction coefficient, $\Delta\chi$ the volume susceptibility anisotropy (the difference between the principal volume susceptibilities parallel and perpendicular to the hydrocarbon-chain direction), V the volume of a crystalline platelet, and H the field strength. As expected from Eq. (3), Kawamura *et al.* [105] have shown that t_R^{-1} varies almost linearly with $H2$ especially in the low-field region. Assuming the thin platelet as an oblate ellipsoid of revolution and evaluating ζ after Perrin [107], they have calculated the value of $\Delta\chi$ from the slope of the line; it is -9×10^{-8} emu/cm^3 (1 JT^{-2}m^{-3} = 10^{-7} emu/cm^3), which corresponds to the molar anisotropy of about -68×10^{-6} emu/mol, assuming the density as 1 g/cm^3, for *L*-DPPC and is -1×10^{-8} emu/cm^3 for PE.

In advance to these works, Boroske and Helfrich [108] estimated the value of $\Delta\chi$ for egg yolk lecithin as -0.27×10^{-8} emu/cm^3 which is an order of magnitude smaller than that for *L*-DPPC. This is elucidated to arise mainly from the different degree-or-ordering of hydrocarbon chains, which are homogeneous and ordered in crystalline *L*-DPPC and inhomogeneous and disordered in egg yolk lecithin in the L_α state [105]. Hydrocarbon chains give enough magnetic anisotropy to thin crystalline platelets of *L*-DPPC and of PE to align them with their hydrocarbon chains perpendicular to the magnetic field. The polar head groups and the planes of the ester bonds in the polar head can give additional contribution to the anisotropy of the magnetic susceptibility.

The curvature-elastic modulus κ of lipid-bilayer has been evaluated by measuring the magnetic-field orientation of the myelin figures of an egg-yolk phosphatidylcholine/water system by Sakurai and Kawamura [109]. The myelin figures are cylindrical rods with concentrically stacked multilamellae of lipid-bilayers in a fully hydrated state. The structural feature of the rods is essentially similar to that of the nerve myelin sheath and the lipid bilayers resemble biomembranes in the structure. They have observed that rod-like myelin figures start to grow from small lumps of hen-egg phosphatidylcholine placed in a plastic cell soon after water was poured into the cell. The myelin figures grow towards the surrounding water and the direction of growth is parallel to the cylindrical axis of the rod. The bilayers of phosphatidylcholine are in a fully hydrated state and there are several types of forms in the rod. Strong optical anisotropy is observed with the optical axis perpendicular to the rod axis. The time needed for growth

saturation depends on the type of the rod. The myelin figures so produced are 5 – 30 μm in diameter and typically no more than 200 μm in length.

They have further shown that upon application of a magnetic field of 0.7 T the myelin figures of simple rod-like form, which grew free into water without touching the inner surface of the plastic cell, become reoriented with their growth axes parallel to the magnetic field within about 10 s possibly through partial bending of each rod near the root. The other rods including various forms of rods take more time to accomplish the magnetic-field reorientation. The bending deformation of the rod is reversible at least within about 10 s or so after the application of the magnetic field. The shape of a reversibly bent rod is determined by equilibrium between the elastic and the magnetic energy densities.

Assuming that bilayers are two dimensional incompressible liquid layers with molecules being perpendicular to the layer plane and the deformation is small, the bending modulus can be related to a curvature-elastic modulus κ of lipid bilayer [110]. From the observed field-induced bending of a myelin figure whose rod was initially perpendicular to the field direction, the value of κ has been evaluated as $4 \cdot 10^{-3}$ erg [109] assuming that the value of $\Delta\chi$ is $-2 \cdot 10^{-9}$ emu/cm^3 [111].

5.4. Sperm Nuclei

The sperm nucleus of a cricket (*G. bimaculatus*) is a rod-like particle with a diameter of 1 μm and a length of 20 μm. It is in a para-crystalline state. Under a magnetic field of 0.88 T. the nuclei of a cricket tend to orient parallel to the field direction exhibiting the birefringence Δn of 1.67×10^{-8}; the induced magnetic-field orientation is due to DNA molecules which are contained by 3 pg in one nucleus and align parallel to the short axis of the rod [67].

5.5. Rhodopsin

Rhodopsin is a visual pigment contained in the visual cells of a vertebrate retina and is a globular chromoprotein (radius about 5 nm) of molecular weight about 40,000. Chagneux and Chalazonitis [101] measured the magnetic-field induced orientation of isolated frog rod

outer segments and Hong [112] estimated the diamagnetic anisotropy of the frog rhodopsin by combining their data with those of diamagnetic anisotropy of lecithin membranes as reported by Boroske and Helfrich [108]. The anisotropy of the volume susceptibilities he has calculated is 4.4×10^{-8} cgs unit/cm^3, which corresponds to 1.5×10^{-27} cgs unit/molecule, or 9.0×10^{-4} cgs unit/mol.

5.6. Fibrinogen

The fibrinogen molecule has a trinodular elongated structure with the length of about 450 Å. Freyssinet *et al.* [113] have observed by accurate birefringence measurements that fibrinogen in dilute solution orients to a small degree under high magnetic fields (maximum field, 13.5 T). This magnetic effect has been explained as due to the molecule having about 30% (by weight) α-helix oriented relatively parallel to the long rod axis. The magnetically induced birefringence varies linearly with H^2 (H, magnetic field strength) up to the highest field used. The birefringence is positive and the long axis of fibrinogen molecule tends to orient in the direction of the magnetic field. The specific Cotton-Mouton constant of fibrinogen is $1.58(\pm 0.1) \times 10^{-7}\,\mathrm{T}^{-2}\,\mathrm{cm}^2\,\mathrm{mg}^{-1}$ and is independent of the protein concentration in the range 10 to 80 mg/ml and of the salt concentration between 0.05 and 0.45 M NaCl. These results demonstrate that over these ranges of conditions there is little intermolecular interaction or significant change in conformation [113]. Highly oriented fibrin results when polymerization takes place slowly in a strong magnetic field.

When fibrin formation is initiated by adding a rate-limiting amount of thrombin to a solution of fibrinogen in a strong magnetic field, the variation of the induced birefringence is sigmoidal [114]. In the early stages fibrinogen molecules and fibrin monomers and origomers have a small diamagnetic anisotropy and consequently their magnetic orientation energy is small compared to kT. However, when large ordered aggregates are formed the magnetic orientation energy becomes sufficiently large enough to surpass the kinetic energy due to the additive property of diamagnetic anisotropy, to give rise to significant orientation and to a large induced birefringence; the gelation starts and proceeds during this process [113].

New fibrin fibers (aggregates) continue to be formed with preferred directionality especially even when the field is cut off beyond a certain critical point since an aligned network has already developed throughout. At near complete orientation, $\Delta n_{sat}/c$ of fibrin gels is $1.24 (\pm 0.07) \times 10^{-5}\,mg^{-1}\,ml$. This value is about 20% of the corresponding values for Pfl and fd [114].

6. MAGNETOTROPISM

When the young shoot of a plant of the higher orders is placed horizontally the lower side of the shoot shows the voltage difference of about 50 mV against the upper side of the shoot, whereas there is no voltage difference between the corresponding sides when it is placed vertically. This effect has been known as the geoelectric effect since long ago and is understood to be caused by the non-uniform distribution of auxine. In order to study the effect of external fields on the behavior of organic substances, Audus [115] constructed a large permanent magnet fitted with pole pieces of triangular cross section that produced a steep magnetic gradient. The gap between a pair of pole pieces is thus not constant. This arrangement gives maximum field strength (0.4 T) just inside the narrowest point (line) of the gap and the steepest gradient ($-56\,T \cdot m^{-1}$) at this line and in an outward direction (in the vertical direction when the field direction is horizontal).

Organic substances are normally weekly diamagnetic. If particles of such materials are placed in a non-uniform magnetic field, a force will be exerted on such particles in the direction of the maximum gradient. This force is given in the form,

$$F = (k_1 - k_2)v \cdot H \cdot (dH/dx) \tag{41}$$

where k_1 and k_2 are the volume susceptibilities of the particle and suspending medium respectively, v is the volume of the particle, H the strength of an external magnetic field, and dH/dx the field gradient.

Audus [115] and Audus and Whish [116] observed the seedling root of cress (*Lepidium sativum*) or the coleoptile of oats (*Avena sativa*) growing on plain 2 per cent agar in a small glass chamber and placed parallel to the gap (between a pair of pole pieces of the magnet) and

slightly above it as near as possible to the region of maximum field gradient. In order to eliminate gravitational effects which might swamp any magnetic effects, the magnet was rotated about the axis of the gap in the dark to eliminate phototropism effects as well. The photographs were taken with synchronized electronic flash illumination of 1 μsec.

In all but a very few cases roots show marked growth curvature away from the gap, that is, down the magnetic gradient. This new plant growth response was named "magnetotropism" by Audus. At present, stimulus receptors for the magnetotropism and for the geotropism are now known; however, the effector system to induce growth bending of the seedling root is considered to be auxine judging from the experimental results concerning the geotropism and phototropism [117]. At any rate, all receptors including the one for the magnetotropism would be in a liquid crystalline state that responds easily to external stimuli.

7. APPLICATIONS

7.1. Production of Ultra-high Modulus Materials

Grigorev *et al.* [118] carried out the comparative study on morphological properties of poly (*p*-phenylene sebacyl di-*p*-hydroxybenzoate) (PPSB),

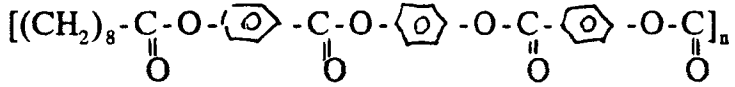

in the solid state and in the melt and became the first to observe the magnetic-field orientation of thermotropic liquid crystals of macromolecules.

The study of highly crystalline polymers aims at developing the technique to produce materials that show mechanical properties equivalent to those shown by metals, of which the flexural modulus of 100 GPa is taken as a representative characteristic. Oda [119] and Nozawa [120] first utilized the phenomenon of magnetic-field orientation of

thermotropic liquid crystals to produce ultra-high modulus polymeric materials. In order to stabilize the diamagnetic field due to the π electrons of a benzene ring, the molecule having this group is apt to align in an external magnetic field so that the induced diamagnetic field becomes perpendicular to the external field, that is, the plane of the benzene ring becomes parallel to the external field. Therefore, polymer molecules having many benzene groups in their main chain like PPSB can orient in an external magnetic field when in liquid crystalline state. The direction of molecular orientation is parallel rather than perpendicular to the magnetic field. This is because the coplanar arrangement of the benzene rings is unstable as in usual macromolecules owing to some steric hindrance and in the latter case only a part of the rings can have the position in which the induced diamagnetic filed is perpendicular to the external field.

Nozawa [120] has tested various polyallylates, polyester amides and polyazomethines in magnetic fields up to 10 T. Rod-like materials moulded under pressure were placed in a magnetic field and heated at a moulding temperature for the predetermined period of time. The materials were then cooled down to room temperature where the orientation of polymer molecules were preserved and were taken out from the field. The torque exerted on the polymer liquid crystals and their magnetic energy acquired in magnetic field are proportional to the square of the field strength. Therefore, the polymer film so prepared becomes more ordered and its flexural modulus increases with the field strength. The value of flexural modulus naturally depends on the time placed in magnetic field. It has been shown that the time required for the projection moulding is within several seconds, whereas that for the magnetic-field moulding is about 20 minutes and that there is a tremendous increase in Young's modulus of the moulded materials in the latter case [120].

When the material is heated at a certain temperature beyond the solid-to-liquid crystal transition temperature prior to put it in magnetic field, the time to reach the equilibrium orientation in magnetic field becomes shorter. The magnetic-field orientation is always achieved as a result of cooperative behavior of molecules that results from the domain structure. This aging effect that depends on the polymeric material has been ascribed to the removal of causes that may prevent the growth of domains [120]. With this moulding method,

the flexural modulus of a commercially available thermotropic liquid-crystalline polymer reaches 50 GPa, whereas it is 10–15 GPa when prepared with the ordinary injection moulding method.

The primary structure of polymer molecules and their mouding weight are important factors in obtaining high modulus products. Using polyazomethine amides,

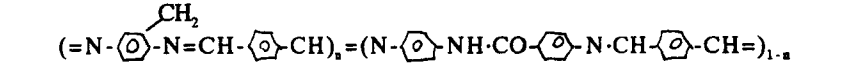

where n is 0.9 or 0.8, Nozawa [120] has been able to produce an ultra-high modulus material, in the magnetic field of 10 T at 200°C for 30 min, that shows the flexural modulus as high as 71 GPa and Oda [119], a polyazomethine fiber (diameter 0.2 mm) that shows the tensile modulus of 101 GPa.

It is generally known that the magnitude of flexural modulus of injection-moulded materials of liquid-crystalline polymers depends on the thickness of the material. The modulus becomes abruptly lower with the thickness since the degree of polymer alignment decreases toward the inside of the material. Materials produced in magnetic field, however, have a uniformly ordered structure regardless of the size and shape of the material, which leads to an ultra-high flexural modulus. Another distinguishing characteristic of the magnetic-field orientation is that it is able to choose the direction of orientation freely. Nozawa [120] has produced a rod of diameter 4 mm in which the polymer chains are perpendicular to the rod axis and a sheet, 1 mm thick, in which the polymer chains are perpendicular to the surface of the sheet using a polyester with flexible spacers and by moulding it in the magnetic field of 1.8 T for 30 min. The rod shows the big difference in light transmissibility between two directions parallel and perpendicular to the rod axis. Meanwhile, the sheet shows excellent transparency.

Ultra-high strength materials in which rigid and flexible polymers are combined in blockwise are known as self reinforced plastics (SRPs). The alignment of polymer molecules is forcibly (mechanically) produced at moulten state where the rigid components are liquid crystalline. Affinity between the two components are usually low and they used to be separated resulting in a non-uniform material. This difficulty can be overcome when rigid polymer is synthesized from its

monomers dissolved in flexible polymer matrix [121]. If the synthesis is carried out in magnetic field, what will be the result of it?

7.2. Control of Molecular Alignment

Trial to control the molecular alignment using magnetic field is not popular unlike that using electric field because of the difficulty in conducting experiments. Piskunov *et al.* [122] has been able to prepare the ordered cell of a thermotropic liquid-crystalline polymer having nitrilo-biphenyl mesogenic side groups,

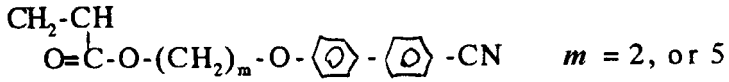

by gradually cooling the polymeric material in the magnetic field of 1.88 T from the isotropic state. The polymer molecules are aligned uniformly in the field direction and polymer membranes so prepared show the different transparency along and perpendicular to the magnetic-field direction. Thermotropic liquid-crystalline polymers are useful compounds for films because of their ability as a gas-barrier and high strength. To minimize the mechanical anisotropy that is inevitable to high-strength materials and causes the film to be easily torn off, the magnetic field effect can be utilized [123].

7.3. Separation of Macromolecules

The force exerted on macromolecules in homogeneous magnetic fields is proportional to the value of magnetic susceptibility. Therefore, concentration gradients of dissolved macromolecules can be produced, if macromolecule and solvent have different magnetic susceptibilities [124]. Since the effective force on the macromolecule is also proportional to $H(dH/dx)$ (H, the field strength), Maret and Dransfeld [11] have suggested that high fields combined with locally high field gradients are useful for obtaining measurable separation effects and hence information about magnetic states and molecular weight even of small macromolecules. Erythrocytes can be almost completely separated in the magnetic field of 1.75 T by the use of the high field gradient

of about $8 \times 10^3 \, T \cdot m^{-1}$ [125]. This separation technique is known by the name of high gradient magnetic separation (HGMS).

In this connection, Haberditzl [124] observed an unexpected increase in activity of an enzyme, *L*-glutamic dehydrogenase, with non-uniform magnetic fields and explained this effect as a secondary effect, namely, the accelerated removal of the paramagnetic oxygen from the site of the reaction.

References

[1] Elliott, A. and Ambrose, E. J. (1950). *Disc. Faraday Soc.*, **9**, 246.
[2] Robinson, C. (1956). *Trans. Faraday Soc.*, **52**, 571.
[3] Robinson, C., Ward, J. C. and Beeveers, R. B. (1958). *Disc. Faraday Soc.*, **25**, 29.
[4] Robinson, C. (1961). *Tetrahedron*, **13**, 219.
[5] Gray, D. G. (1983). *J. Appl. Polymer Sci. Symp.*, **37**, 179.
[6] Flory, P. J. (1956). *Proc. Roy. Soc. (London)*, **A234**, 73.
[7] Alberts, B., Dennis, B., Lewis, J. *et al.* (1983). "Molecular Biology of the Cell", *Garland Pub. Inc.*, New York.
[8] Jackson, W. J. Jr. and Kuhfuss, H. F. (1976). *J. Polymer Sci. Chem.*, **14**, 2043.
[9] McFarlane, F. E., Nicely, V. A. and Davis, T. G. (1977). In: "Contemporary Topics in Polymer Science", Pierce, E. M. and Schaefgan, J. R., Eds., *Plenum*, **2**, 109.
[10] Maret, G. V., Schickfus, M., Mayer, A. *et al.* (1975). *Phys. Review Letters*, **35**, 397.
[11] Maret, G. and Dransfeld, K. (1977). *Physica*, **86–88B**, 1077.
[12] Gans, R. (1921). *Ann. Phys. (Leipzig)*, **64**, 481.
[13] Le Fevre, R. J. M. (1965). *Adv. Phys. Org. Chem.*, **3**, 1.
[14] Hermans, J. Jr. (1962). *J. Colloid Sci.*, **17**, 638.
[15] Sobajima, S. (1967). *J. Phys. Soc. Japan*, **23**, 1070.
[16] Panar, M. and Phillips, W. D. (1968). *J. Am. Chem. Soc.*, **90**, 3880.
[17] Gill, D., Klein, M. P. and Kotowycz, G. (1968). *J. Am. Chem. Soc.*, **90**, 6870.
[18] Orwoll, R. D. and Vold, R. L. (1971). *J. Am. Chem. Soc.*, **93**, 5335.
[19] Hiraoki, T., Tsutsumi, A., Hikichi, K. *et al.* (1975). *Polymer J.*, **7**, 507.
[20] Iizuka, E. (1973). *Polymer J.*, **5**, 62.
[21] Gutowsky, H. S. and Pake, G. E. (1950). *J. Chem. Phys.*, **18**, 162.
[22] Spence, R. D., Moses, H. A. and Jain, P. L. (1953). *J. Chem. Phys.*, **21**, 380.
[23] Spence, R. D., Gutowsky, H. S. and Holm, C. H. (1953). *J. Chem. Phys.*, **21**, 1891.
[24] Jain, P. L., Lee, J. C. and Spence, R. D. (1955). *J. Chem. Phys.*, **23**, 878.
[25] Iizuka, E. and Go, Y. (1971). *J. Phys. Soc. Japan* (1971) **13**, 1205.
[26] Tsuboi, M. (1962). *J. Polymer Sci.*, **59**, 139.
[27] Iizuka, E. (1971). *Biochim. Biophys, Acta*, **243**, 1.
[28] Iizuka, E. (1976). In: "Advances in Polymer Science Vol. 20", Cantow, H. J. *et al.* Eds. Springer-Verlag, pp. 79–107.
[29] Iizuka, E. (1974). *Mol. Cryst. Liq. Cryst.*, **27**, 161.
[30] Wada, A. (1959). *J. Chem. Phys.*, **30**, 328.
[31] Iizuka, E. (1969). *Biochim. Biophys. Acta*, **175**, 457.
[32] Iizuka, E. (1988). *Adv. Biophys.*, **24**, 1.
[33] Iizuka, E. (1985). *J. Appl. Polymer Sci. Symp.*, **41**, 131.
[34] Ornstein, L. S. and Kast, W. (1927). *Trans. Faraday Soc.*, **29**, 931.
[35] Peterlin, A. and Stuart, H. A. (1939). *Z. Physik*, **112**, 129.
[36] Go, Y., Ejiri, S. and Fukada, E. (1969). *Biochim. Biophys. Acta*, **175**, 454.

[37] Murthy, N. S., Samulski, E. T. and Knox, J. R. (1986). *Macromolecules*, **19**, 941.
[38] Mckinnon, A. J. and Tobolsky, A. V. (1966). *J. Phys. Chem.*, **70**, 1453.
[39] Iizuka, E., Keira, T. and Wada, A. (1973). *Mol. Cryst. Liq. Cryst.*, **23**, 13.
[40] Toth, W. J. and Tobolsky, A. V. (1970). *Polymer Letters*, **8**, 537.
[41] Wilkes, G. L. (1972). *Mol. Cryst. Liq. Cryst.*, **18**, 165.
[42] Go, Y. and Kubo, T. (1936). *J. Soc. Chem. Ind. Jpn.*, **39**, 929.
[43] Honda, M., Suzuki, H. and Kato, T. (1971). *Repts. Progr. Polymer Phys. Jpn.*, **14**, 607.
[44] Samulski, E. T. and Tobolsky, A. V. (1968). *Macromolecules*, **1**, 555.
[45] Samulski, E. T. and Tobolsky, A. V. (1971). *Biopolymers*, **10**, 1013.
[46] Guha Sridhar, C., Hines, W. A. and Sumulski, E. T. (1974). *Chem. Phys.*, **61**, 947.
[47] Yomosa, S. (1970). In: "*Proceedings of the 9th Annual Meeting of Biophysical Society of Japan*", 1-C-8p.
[48] Samulski, E. T. and Berendsen, J. C. (1972). *J. Chem. Phys.*, **56**, 3920.
[49] Miyata, N., Tohyama, K. and Go, Y. (1972). *J. Phys. Soc. Japan*, **33**, 1180.
[50] Finer, E. G. and Darke, A. (1975). *Faraday Trans.*, I. **71**, 984.
[51] Pauling, L. (1960). "The Nature of the Chemical Bond", Cornell Univ. Press, Ithaca, New York, 3rd edn., p. 282.
[52] Pauling, L. (1979). *Proc. Natl. Acad. Sci. USA*, **76**, 2293.
[53] Tohyama, K. and Miyata, N. (1973). *J. Phys. Soc. Japan*, **34**, 1699.
[54] Tohyama, K. and Miyata, N. (1974). *Mol. Cryst. Liq. Cryst.*, **29**, 35.
[55] Tohyama, K. and Iizuka, E. (1974). *J. Phys. Soc. Jpn.*, **37**, 1172.
[56] Meyer, R. B. (1968). *Appl. Phys. Letters*, **12**, 281.
[57] Frank, F. C. (1958). *Disc. Faraday Soc.*, **25**, 19.
[58] de Gennes, P. G. (1968). *Solid State Commun.*, **6**, 163.
[59] Duke, R. W. and DuPrè, D. B. (1974). *J. Chem. Phys.*, **60**, 2759.
[60] Toriumi, H., Matsuzawa, K. and Uematsu, I. (1984). *J. Chem. Phys.*, **81**, 6085.
[61] Kihara, H. (1977). *Polymer J.*, **9**, 443.
[62] Straley, J. P. (1973). *Mol. Cryst. Liq. Cryst.*, **22**, 333.
[63] DuPrè, D. B., and Duke, R. W. (1975). *J. Chem. Phys.*, **63**, 143.
[64] Duke, R. W., DuPrè, D. B. and Samulski, E. T. (1977). *J. Chem. Phys.*, **66**, 2748.
[65] Iizuka, E. and Yang, J. T. (1978). In: "Liquid Crystals and Ordered Fluids Vol. 3", Johnson, J. F. and Porter, R. S. Eds., Plenum., New York, p. 207.
[66] Astbury, W. T. (1947). In: "*Symp. Soc. Exp. Biol., I. Nucleic Acid*", University Press, Cambridge, p. 66.
[67] Suzuki, S. and Wakabayashi, K. (1984). In: "KEK", Nakajima, T. Ed., **83–23**, 7.
[68] Rhodes, M. B. and Stein, R. B. (1969). *J. Polymer Sci. A-2*, **7**, 1539.
[69] Rich, A. and Kasha, M. (1960). *J. Am. Chem. Soc.*, **82**, 6197.
[70] Iizuka, E. and Kondo, Y. (1979). *Mol. Cryst. Liq. Cryst.*, **51**, 285.
[71] Sutherland, G. B. B. M. and Tsuboi, M. (1957). *Proc. Royal. Soc.*, **A239**, 446.
[72] Peterlin, A. and Stuart, A. (1939). *Z. Physik*, **112**, 129.
[73] Iizuka, E. (1978). *Polymer J.*, **10**, 293.
[74] Roviello, A. and Sirigu, A. (1982). *Makromol. Chem.*, **183**, 895.
[75] Finkelmann, H., Happ, M., Portugal, M. *et al.* (1978). *Macromol. Chem.*, **179**, 2541.
[76] Hsu, E. C., Clough, S. B. and Blumstein, A. (1977). *J. Polymer Sci. Lett.*, **15**, 545.
[77] Blumstein, A. (1978). "Liquid Crystalline Order in Polymers", Academic Press.
[78] Volino, F., Martins, A. F. and Blumstein, R. B. (1981). *J. Physique Lett.*, **42**, L-305.
[79] Liebert, L., Strzelecki, L., Van Luyen, D. *et al.* (1981). *Eur. Polymer J.*, **17**, 71.
[80] Hardouin, F., Achard, M. F. and Gasparoux, H. (1982). *J. Polymer Sci. Phys.*, **20**, 975.
[81] de Gennes, P. G. (1975). *C. R. Acad. Sci. B*, **281**, 101.
[82] Regaya, B. and Gasparoux, H. C. R. (1971). *Acad. Sci.*, **272B**, 724.
[83] Noel, C., Monnerie, L., Achard, M. F. *et al.* (1981). *Polymer*, **22**, 578.

[84] Achard, M. F., Hardouin, F., Sigaud, G. *et al.* (1976). *J. Chem. Phys.*, **65**, 1387.
[85] Kasuya, S., Sasaki, S., Watanabe, J. *et al.* (1982). *Polymer Bull.*, **7**, 241.
[86] Hanabusa, K., Sato, M., Shirai, H. *et al.* (1984). *J. Polymer Sci. Lett.*, **22**, 559.
[87] Hanabusa, K., Yanagisawa, K., Higashi, J. *et al.* (1990). *J. Polymer Sci. Chem.*, **28**, 825.
[88] Iizuka, E. and Iida, S. (1990). *Polymer J.*, **22**, 628.
[89] Iizuka, E., Kiriki, T. and Abe, K. (1991). *Polymer J.*, **23**, 1507.
[90] Pople, J. A. (1956). *J. Chem. Phys.*, **24**, 1111.
[91] Elliott, G. F. and Rome, E. M. (1969). In: "Liquid Crystals", Brown, G. H., Ed., Gordon and Breach, New York, **2**, Part II, p. 383.
[92] Finch, J. T., Perutz, M. F., Bertles, J. F. *et al.* (1973). *Proc. Nat'l. Acad. Sci. USA*, **70**, 718.
[93] Bertles, J. F., Rabinowitz, R. and Doebler, J. (1970). *Science*, **169**, 375.
[94] Taylor, D. S. and Coryell, C. A. (1938). *J. Am. Chem. Soc.*, **60**, 1177.
[95] Murayama, M. (1966). *Science*, **153**, 145.
[96] Iizuka, E. (1977). *Mol. Cryst. Liq. Cryst.*, **42**, 67.
[97] Torbet, J. and Maret, G. (1981). *Biopolymers*, **20**, 2657.
[98] Makowski, L., Caspar, D. L. D. and Marvin, D. A. (1980). *J. Mol. Biol.*, **140**, 149.
[99] Marvin, D. A. (1966). *J. Mol. Biol.*, **15**, 8.
[100] Stanley, W. M. (1935). *Science*, **81**, 644.
[101] Chagneux, R. and Chalazonitis, N. (1972). *C. R. Acad. Sci. D*, **274**, 317.
[102] Becker, J. F., Geacintov, N. E., Van Nostrand, F. *et al.* (1973). *Biochim. Biophys. Commun.*, **51**, 597.
[103] Sakurai, I., Kawamura, Y., Ikegami, A. *et al.* (1980). *Proc. Nat'l. Acad. Sci. USA*, **77**, 7232.
[104] Lonsdale, K. (1939). *Proc. Soc. London*, **A171**, 541.
[105] Kawamura, Y., Sakurai, I. and Ikegami, A. (1981). *Mol. Cryst. Liq. Cryst.*, **67**, 77.
[106] Hong, F. T. (1977). *J. Colloid Interface Sci.*, **58**, 471.
[107] Perrin, F. (1934). *J. Phys. Radium Ser. 7*, **5**, 499.
[108] Boroske, E. and Helfrich, W. (1978). *Biophys. J.*, **24**, 863.
[109] Sakurai, I. and Kawamura, Y. (1983). *Biochim. Biophys. Acta*, **735**, 189.
[110] Helfrich, W. (1973). *Z. Naturforsch.*, **28c**, 693.
[111] Kawamura, Y., Sakurai, I. and Iwayanagi, S. (1983). *Rept. Progr. Polym. Phys. Japan.*, **26**, 743.
[112] Hong, F. T. (1980). *Biophys. J.*, **29**, 343.
[113] Freyssinet, J.-M., Torbet, J. and Hudry-Clergeon, G. (1983). *Proc. Nat'l. Acad. Sci. USA*, **80**, 1616.
[114] Torbet, J., Freyssinet, J.-M. and Hudry-Clergeon, G. (1981). *Nature*, **289**, 91.
[115] Audus, L. J. (1960). *Nature*, **185**, 132.
[116] Audus, L. J. and Whish, J. C. (1964). "Biological Effects of Magnetic Fields", Plenum Press, New York.
[117] Suzuki, H. and Honda, M. (1970). *Biophysics*, **10**, 205 (in Japanese).
[118] Grigorev, A. I., Andreeva, N. A., Bilibin, A. Yu. *et al.* (1980). *Vysokomol. Soedin., Ser. B*, **22**, 891.
[119] Oda, F. (1986). In: "*Proceedings of the 4th Symposium*", Research Association for Basic Polymer Technology (Ed.) Sections 8, 9 (in Japanese).
[120] Nozawa, S. (1991). In: "*Proceedings of the 9th Symposium*", Research Association for Basic Polymer Technology (Ed.) Sections 2, 3 (in Japanese).
[121] Ogata, N., Sanui, K. and Itaya, H. (1990). *Polymer J.*, **22**, 85.
[122] Piskunov, M. V., Kostromin, S. G., Stroganov, L. B. *et al.* (1982). *Makromol. Chem. Commun.*, **3**, 443.
[123] Jpn. Pat. S63-242513 (Sumitomo Bakelite).
[124] Haberditzl, W. (1967). *Nature*, **13**, 72.
[125] Melville, D., Paul, F. and Roath, S. (1975). *Nature*, **255**, 706.